SIAM J. NUMER. ANAL.
Vol. 37, No. 6, pp. 1768–1799

THE FINITE MASS METHOD*

CHRISTOPH GAUGER†, PETER LEINEN†, AND HARRY YSERENTANT†

Abstract. The finite mass method, a new Lagrangian method for the numerical simulation of gas flows, is presented and analyzed. In contrast to the finite volume and the finite element method, the finite mass method is founded on a discretization of mass, not of space. Mass is subdivided into small mass packets of finite extension, each of which is equipped with finitely many internal degrees of freedom. These mass packets move under the influence of internal and external forces and the laws of thermodynamics and can undergo arbitrary linear deformations. The method is based on an approach recently developed by Yserentant and can attain a very high accuracy.

Key words. finite mass method, gridless discretizations, compressible fluids

AMS subject classifications. 76N99, 76M25, 65M99

PII. S0036142999352564

1. Introduction.

Fluid mechanics is usually stated in terms of conservation laws that link the change of a quantity like mass or momentum inside a given volume to a flux of this quantity across the boundary of the volume. The finite volume method is directly based on this formulation. Space is subdivided into little cells, and the balance laws for mass, momentum, and energy are set up for each of these cells separately. Similarly, the finite element method is based on a discretization of space and a choice for the trial functions on the resulting cells.

In contrast, the finite mass method is founded on a discretization of mass, an idea which is at least as obvious and that can be traced back to the work of von Neumann [10] or Pasta and Ulam [9] in the late 1940s and the 1950s. Instead of dividing space into elementary cells, we divide mass into a finite number of mass packets of finite extension, each of which is equipped with a given number of internal degrees of freedom. These mass packets move under the influence of internal and external forces and the laws of thermodynamics and can intersect and penetrate each other. They can contract, expand, rotate, and even change their shape. Their internal mass distribution is described by a fixed shape function, similarly to finite elements. Although the finite mass method is a purely Lagrangian approach, it has not much to do with particle methods as they are used for Boltzmann-like transport equations; in some way, it is much closer to finite element and finite volume schemes. The approximations it produces are differentiable functions and not discrete measures. The method is basically of second order, and in some experiments we observed even fourth order convergence!

The Lagrangian form of description of fluid flows can have many advantages. For example, there are no problems with free surfaces and no convection terms arise. Such features make numerical methods based on the Lagrangian view especially attractive for free flows in unbounded space. In fact, one of the most popular methods of this type, Monaghan's smoothed particle hydrodynamics [8], has its origins in astrophysics. Like the smoothed particle hydrodynamics, the finite mass method is a completely

*Received by the editors February 16, 1999; accepted for publication (in revised form) November 3, 1999; published electronically May 23, 2000.
http://www.siam.org/journals/sinum/37-6/35256.html
†Mathematisches Institut der Universität Tübingen, 72076 Tübingen, Germany (yserentant@na.uni-tuebingen.de).

grid-free approach, but it is not a method de facto imitating statistical mechanics and possesses a sounder mathematical and physical foundation.

The finite mass method is a generalization and extension of the particle model of compressible fluids that had been proposed by Yserentant in [11], [12], and [13] and is based on the principles developed there. The compactness and convergence results obtained in [11] and [13] concerning the transition to the continuum limit transfer to the present situation. In contrast to the approach in the articles mentioned above, the single mass packets can now undergo arbitrary linear deformations and not only rotations and changes of size. Although the dimension of the configuration manifold of the single mass packet increases because of that, this strongly simplifies the equations of motion the mass packets are subject to because the configuration manifold is now a linear space. The equations of motion take the same form for all space dimensions. The main advantages, however, are the superior approximation properties, due to the fact that the mass packets can now be deformed by the flow.

The main issue with a method like ours is how the equations of motion for the mass packets or particles, as we often prefer to say, are set up. We start from the basic physical principles that finally lead to the Euler and Navier–Stokes equations, not from these equations themselves and a least squares or Galerkin approach. In consequence, the equations of motion also do not break down when particles completely cover each other. In the most simple case of an adiabatic, inviscid flow, the equations of motion for the particles are derived from a Lagrange-function with the internal energy as potential energy. To damp the fluctuation part of the local kinetic energy that necessarily arises with every such model, frictional forces vanishing in the limit of particle sizes tending to zero are added to these potential forces. They break the invariance to time reversal and make the method consistent with the second law of thermodynamics.

The paper is organized as follows. In section 2, the finite mass method is explained and derived in detail, both for inviscid and for viscous fluids. It is shown how the mass density, the velocity field, and, as second independent thermodynamic quantity, the entropy are discretized. The sort of approximation properties that can be expected is discussed. The equations of motion describing the local interaction of the mass packets and the time evolution of the system are set up. A main feature of the approach is that mass, momentum, angular momentum, and energy are exactly conserved. The conservation of mass follows immediately from the construction and is discussed in section 2. The conservation of energy, momentum, and angular momentum is studied in section 3. The conservation of angular momentum is a remarkable fact because in continuum mechanics the conservation of angular momentum is hidden in the symmetry of the stress tensor and does not appear explicitly as a conservation law. Consequently, most discretizations violate this principle.

The finite mass method as described in section 2 is invariant to arbitrary translations and rotations, and, as it concerns the shape the mass packets can attain, even to every linear transformation of space. These properties are reflected by the quadrature formulas that are developed in section 4 to evaluate the integrals which define the forces acting upon the particles. Conservation of momentum, angular momentum, and energy are maintained. In section 4, we also discuss how the forces and moments acting upon the particles can be calculated on the computer.

In section 5, a suitable time discretization is presented. The proposed scheme is an exponential integrator in the spirit of the recent paper [4] by Hochbruck and Lubich. In case of pure pressure forces, it transfers to the well-known Störmer–Verlet

method for second order equations and conserves momentum and angular momentum exactly.

Finally, in section 6, some typical test calculations for flows in two space dimensions are documented. These examples clearly demonstrate the potential and the high accuracy of the method.

We restrict our attention in this article to free flows in vacuum. Their treatment of boundaries will be the subject of a forthcoming paper. Simple reflection laws for particles touching the walls of bounded volumes have already been given in [11], [12], and [13].

For a certain background in mechanics and fluid dynamics, we refer to the textbooks [5], [6] by Landau and Lifschitz, to the book [1] by Chorin and Marsden, and to the classical monograph [2] by Courant and Friedrichs.

2. The particle model of compressible fluids. The basic ingredient of the finite mass method is a continuously differentiable shape function $\psi : \mathbb{R}^d \to \mathbb{R}$, d the space dimension, with compact support that attains only values ≥ 0. This function describes the internal mass distribution inside the mass packets into which the fluid is subdivided. We assume that

$$\int \psi(\mathbf{y})\,\mathrm{d}\mathbf{y} = 1, \quad \int \psi(\mathbf{y})\mathbf{y}\,\mathrm{d}\mathbf{y} = \mathbf{0}. \tag{2.1}$$

The second property states that the origin of the body coordinate system attached to a particle is its center of mass. Further we suppose that

$$\int \psi(\mathbf{y})\, y_k y_l\,\mathrm{d}\mathbf{y} \;=\; J\,\delta_{kl}, \tag{2.2}$$

with the y_k the components of $\mathbf{y}$.

For example, the function ψ may be built up from a piecewise polynomial function $\widetilde{\psi} : \mathbb{R} \to \mathbb{R}_+$ in one space variable. If we let

$$\psi(\mathbf{y}) = \prod_{k=1}^{d} \widetilde{\psi}(y_k), \tag{2.3}$$

the conditions (2.1) are equivalent to

$$\int \widetilde{\psi}(\xi)\,\mathrm{d}\xi = 1, \quad \int \widetilde{\psi}(\xi)\xi\,\mathrm{d}\xi = 0. \tag{2.4}$$

The second condition in (2.4) also implies that the integrals (2.2) vanish for $k \neq l$. The constant J is given by

$$J = \int \widetilde{\psi}(\xi)\xi^2\,\mathrm{d}\xi \tag{2.5}$$

and does not depend on the space dimension. A suitable choice for $\widetilde{\psi}$, which we have used in the numerical computations documented in section 6, is the normalized third order B-spline given by

$$\widetilde{\psi}(\xi) = \frac{4}{3}\begin{cases} 2\,(1+\xi)^3, & -1 \leq \xi \leq -1/2, \\ 1-6\xi^2(1+\xi), & -1/2 \leq \xi \leq 0, \\ 1-6\xi^2(1-\xi), & 0 \leq \xi \leq 1/2, \\ 2\,(1-\xi)^3, & 1/2 \leq \xi \leq 1, \end{cases} \tag{2.6}$$

for $|\xi| \leq 1$ and by $\widetilde{\psi}(\xi) = 0$ for $|\xi| > 1$. It can be composed of smaller copies and be used to build up a basis for the cubic spline functions on a uniform grid. This $\widetilde{\psi}$ fulfills the conditions (2.4), and the constant (2.5) takes the value

$$J = \frac{1}{12}. \tag{2.7}$$

An advantage of such tensor product-like shape functions, are their good approximation properties.

The points $\mathbf{y}$ of the particle i move along the trajectories

$$t \;\rightarrow\; \mathbf{q}_i(t) + \mathbf{H}_i(t)\mathbf{y}, \quad \det \mathbf{H}_i(t) > 0. \tag{2.8}$$

The vector $\mathbf{q}_i(t)$ determines the position of the particle, and the matrix $\mathbf{H}_i(t)$ determines its size, shape, and orientation in space. Correspondingly,

$$\mathbf{y} \;=\; \mathbf{H}_i(t)^{-1}(\mathbf{x}-\mathbf{q}_i(t)) \tag{2.9}$$

are the body coordinates of the point at position $\mathbf{x}$ in space at time t. Let $m_i > 0$ denote the mass of the particle i. The total mass density

$$\rho(\mathbf{x},t) = \sum_{i=1}^{N} m_i \,[\det \mathbf{H}_i(t)]^{-1} \psi\big(\mathbf{H}_i(t)^{-1}(\mathbf{x}-\mathbf{q}_i(t))\big) \tag{2.10}$$

then results from the superposition of the mass densities of the single particles.

The points $\mathbf{y}$ of the particle i have the velocity

$$t \;\rightarrow\; \mathbf{q}_i'(t) + \mathbf{H}_i'(t)\mathbf{y}. \tag{2.11}$$

Inserting the expression (2.9) for $\mathbf{y}$, one gets the velocity field

$$\mathbf{v}_i(\mathbf{x},t) = \;\mathbf{q}_i'(t) + \mathbf{H}_i'(t)\mathbf{H}_i(t)^{-1}(\mathbf{x}-\mathbf{q}_i(t)) \tag{2.12}$$

of the particle i related to the space coordinates. The total mass flux density

$$\mathbf{j}(\mathbf{x},t) = \sum_{i=1}^{N} m_i \,[\det \mathbf{H}_i(t)]^{-1} \psi\big(\mathbf{H}_i(t)^{-1}(\mathbf{x}-\mathbf{q}_i(t))\big)\, \mathbf{v}_i(\mathbf{x},t) \tag{2.13}$$

again results from the superposition of the mass flux densities of the single particles. With the local mass fractions

$$\chi_i(\mathbf{x},t) = \;\frac{m_i \,[\det \mathbf{H}_i(t)]^{-1} \psi\big(\mathbf{H}_i(t)^{-1}(\mathbf{x}-\mathbf{q}_i(t))\big)}{\rho(\mathbf{x},t)}, \tag{2.14}$$

the velocity field $\mathbf{v}$ of the flow, which is defined by the relation

$$\mathbf{j}(\mathbf{x},t) = \rho(\mathbf{x},t)\mathbf{v}(\mathbf{x},t), \tag{2.15}$$

is the convex combination

$$\mathbf{v}(\mathbf{x},t) = \sum_{i=1}^{N} \chi_i(\mathbf{x},t)\mathbf{v}_i(\mathbf{x},t) \tag{2.16}$$

of the velocity fields of the single particles.

To simplify notation, we introduce the abbreviation

$$\psi_i \;=\; [\det \mathbf{H}_i]^{-1}\psi\big(\mathbf{H}_i^{-1}(\mathbf{x}-\mathbf{q}_i)\big) \;=\; [\det \mathbf{H}_i]^{-1}\psi(\mathbf{y}), \tag{2.17}$$

where again $\mathbf{y} = \mathbf{H}_i^{-1}(\mathbf{x}-\mathbf{q}_i)$. The gradient of ψ_i, which is the derivative of ψ_i with respect to $\mathbf{x}$, is

$$\nabla\psi_i \;=\; [\det \mathbf{H}_i]^{-1}\mathbf{H}_i^{-\mathrm{T}}(\nabla\psi)(\mathbf{y}) \tag{2.18}$$

and can, as the derivatives

$$\frac{\partial\psi_i}{\partial\mathbf{q}_i} \;=-\nabla\psi_i, \quad \frac{\partial\psi_i}{\partial\mathbf{H}_i} \;=-[\nabla\psi_i][\,\mathbf{y}\,]^{\mathrm{T}}-\psi_i\mathbf{H}_i^{-\mathrm{T}}, \tag{2.19}$$

be expressed in terms of the internal variables $\mathbf{y}$.

To derive the expression above for the derivative with respect to the matrix $\mathbf{H}_i$, we suppress the index i serving for the distinction of the particles and write ψ^* instead of ψ_i. First we observe that, for $\mathbf{H}$ fixed and $\mathbf{E}$ tending to zero,

$$(\mathbf{H}+\mathbf{E})^{-1} \;=\; (\mathbf{I}+\mathbf{H}^{-1}\mathbf{E})^{-1}\mathbf{H}^{-1} \;=\; (\mathbf{I}-\mathbf{H}^{-1}\mathbf{E})\mathbf{H}^{-1} \,+\, o(\mathbf{E})$$

and, because of

$$\det(\mathbf{I}+\mathbf{A}) \;=\; 1+\mathrm{tr}\mathbf{A}+o(\mathbf{A})$$

for $\mathbf{A}$ tending to zero, similarly

$$\det(\mathbf{H}+\mathbf{E}) \;=\; (\det\mathbf{H})(1+\mathbf{H}^{-\mathrm{T}}\cdot\mathbf{E})+o(\mathbf{E})\,,$$

where

$$\mathbf{A}\cdot\mathbf{B} \;=\; \sum_{k,l}\mathbf{A}|_{kl}\mathbf{B}|_{kl} \;=\; \mathrm{tr}(\mathbf{A}^{\mathrm{T}}\mathbf{B})$$

denotes the inner product of two matrices $\mathbf{A}$ and $\mathbf{B}$. One finds

$$\begin{aligned}&\frac{1}{\det(\mathbf{H}+\mathbf{E})}\;\psi\big((\mathbf{H}+\mathbf{E})^{-1}(\mathbf{x}-\mathbf{q})\big)\\ &\qquad=\;\frac{1-\mathbf{H}^{-\mathrm{T}}\cdot\mathbf{E}}{\det\mathbf{H}}\;\psi(\mathbf{y})\;-\;\frac{1}{\det\mathbf{H}}\;(\nabla\psi)(\mathbf{y})\cdot\mathbf{H}^{-1}\mathbf{E}\mathbf{y}\;+\;o(\mathbf{E}).\end{aligned}$$

This means that the linear mapping

$$\mathbf{E}\;\to\;-\,\frac{1}{\det\mathbf{H}}\;\mathbf{H}^{-\mathrm{T}}(\nabla\psi)(\mathbf{y})\cdot\mathbf{E}\mathbf{y}\;-\;\frac{\mathbf{H}^{-\mathrm{T}}\cdot\mathbf{E}}{\det\mathbf{H}}\;\psi(\mathbf{y})$$

is the total derivative of

$$\mathbf{H}\;\to\;\frac{1}{\det\mathbf{H}}\;\psi\big(\mathbf{H}^{-1}(\mathbf{x}-\mathbf{q})\big)$$

at given $\mathbf{H}$. Inserting $\mathbf{E}|_{\nu\mu}=\delta_{k\nu}\delta_{l\mu}$ for the entries of $\mathbf{E}$ and using (2.17), (2.18),

$$\frac{\partial\psi^*}{\partial\mathbf{H}}\,\Big|_{kl} = -[\nabla\psi^*][\,\mathbf{y}\,]^{\mathrm{T}}-\psi^*\mathbf{H}^{-\mathrm{T}}\,\Big|_{kl}$$

follows.

The continuity equation expressing the conservation of mass is automatically satisfied with the given ansatz. Independently of the size and shape of the particles and their distribution in space,

$$\frac{\partial \rho}{\partial t} + \operatorname{div}(\rho \mathbf{v}) = 0. \tag{2.20}$$

This follows from the fact that such an equation holds for every single particle, as one proves using (2.19) and $\operatorname{div} \mathbf{v}_i = \mathbf{H}_i^{-\mathrm{T}} \cdot \mathbf{H}_i'$.

To study the potential accuracy of the approach, we start from a given twice continuously differentiable velocity field $\mathbf{u}$. Then fixing the particle trajectories $\mathbf{q}_i(t)$ and the matrices $\mathbf{H}_i(t)$ for $t \geq t_0$, with given initial values, as solutions of the differential equations

$$\mathbf{q}_i'(t) = \mathbf{u}(\mathbf{q}_i(t), t), \quad \mathbf{H}_i'(t) = (\nabla \mathbf{u})(\mathbf{q}_i(t), t)\, \mathbf{H}_i(t), \tag{2.21}$$

the velocity field (2.12) of the particle i reads

$$\mathbf{v}_i(\mathbf{x}, t) = \mathbf{u}(\mathbf{q}_i(t), t) + (\nabla \mathbf{u})(\mathbf{q}_i(t), t)(\mathbf{x} - \mathbf{q}_i(t)) \tag{2.22}$$

and is therefore a second order approximation of $\mathbf{u}$ in a neighborhood of $\mathbf{x} = \mathbf{q}_i(t)$. As the mass fractions (2.14) form a partition of unity, the resulting overall velocity field

$$\mathbf{v}(\mathbf{x}, t) = \mathbf{u}(\mathbf{x}, t) + \sum_{i=1}^{N} \chi_i(\mathbf{x}, t)(\mathbf{v}_i - \mathbf{u})(\mathbf{x}, t) \tag{2.23}$$

remains a second order approximation of $\mathbf{u}$ on the region occupied by mass, independent of where the particles are located. The mass density is an exact solution of the transport equation (2.20) with respect to this perturbed velocity field and therefore, with corresponding initial values, a good approximation of the true density in the sense of a backward error analysis. For a more careful and detailed analysis of this type also covering the motion in an external force field, we refer to [14].

For a complete description of the thermodynamic state of a compressible fluid, aside from the mass density ρ, a second thermodynamic quantity like temperature is needed. Most convenient for our purposes is the entropy density s that is given here in the form

$$s(\mathbf{x}, t) = \sum_{i=1}^{N} S_i(t) m_i \, [\det \mathbf{H}_i(t)]^{-1} \psi\big(\mathbf{H}_i(t)^{-1}(\mathbf{x} - \mathbf{q}_i(t))\big), \tag{2.24}$$

where the $S_i(t)$ denote the specific entropies of the single particles. In particular, the specific entropy

$$S(\mathbf{x}, t) = \frac{s(\mathbf{x}, t)}{\rho(\mathbf{x}, t)} \tag{2.25}$$

is the convex combination

$$S(\mathbf{x}, t) = \sum_{i=1}^{N} S_i(t) \chi_i(\mathbf{x}, t) \tag{2.26}$$

of the specific entropies of the single particles. As with the velocity, one recognizes that this representation potentially leads to a first order approximation of the exact specific entropy independent of the distribution of the particles, where the actual accuracy can again be much higher.

The pressure, the absolute temperature, and the internal energy per unit volume

$$\pi(\rho,s),\quad \theta(\rho,s),\quad \varepsilon(\rho,s) \tag{2.27}$$

are functions of the mass density and the entropy density. These functions are not independent of each other but are connected by the Gibbs fundamental relation of thermodynamics taking the form

$$\pi = \frac{\partial\varepsilon}{\partial\rho}\rho + \frac{\partial\varepsilon}{\partial s}s - \varepsilon, \quad \theta = \frac{\partial\varepsilon}{\partial s} \tag{2.28}$$

in the present variables. We assume that the internal energy $\varepsilon(\rho,s)$ is defined for all $\rho > 0$ and all real s and is twice continuously differentiable on this set. We suppose that

$$\varepsilon > 0, \quad \frac{\partial\varepsilon}{\partial s} > 0 \tag{2.29}$$

for all these ρ and s and require that ε/ρ and the first order partial derivatives of ε can be extended by the value 0 at $(\rho,s) = (0,0)$ to functions that are continuous on the sectors $|s| \le S^*\rho$, $S^* > 0$. Barytropic ideal gases with

$$\varepsilon(\rho,s) = \frac{\pi_0}{\gamma-1}\Big(\frac{\rho}{\rho_0}\Big)^\gamma \exp\Big(\frac{1}{c_v}\frac{s}{\rho}\Big), \tag{2.30}$$

represent a simple example. The constant $\pi_0 > 0$ is a characteristic pressure, the constant $\rho_0 > 0$ a characteristic mass density, and the constant $c_v > 0$ the characteristic heat for constant volume. The constant $\gamma > 1$ is the ratio of the specific heats for constant pressure and constant volume. A typical value is $\gamma = 1.4$ for air.

The particle i has the kinetic energy

$$E_i(t) = \frac{1}{2}\int m_i\,\psi_i(\mathbf{x},t)|\mathbf{v}_i(\mathbf{x},t)|^2\,\mathrm{d}\mathbf{x} \tag{2.31}$$

that attains the closed representation

$$E_i = \frac{1}{2}m_i|\mathbf{q}_i'|^2 + \frac{1}{2}Jm_i|\mathbf{H}_i'|^2, \tag{2.32}$$

where $|\cdot|$ denotes the Euclidean norm of a vector and the Frobenius norm of a matrix, respectively. The total kinetic energy of the system is

$$E(t) = \sum_{i=1}^{N} E_i(t). \tag{2.33}$$

From the kinetic energy (2.33) and the internal energy

$$V = \int \varepsilon(\rho(\mathbf{x},t),s(\mathbf{x},t))\,\mathrm{d}\mathbf{x}, \tag{2.34}$$

the Lagrange-function

$$\mathcal{L} = E - V \tag{2.35}$$

of the system is formed. For the completely adiabatic case that is described by the Euler-equations of gas dynamics, the equations of motion

$$\frac{\mathrm{d}}{\mathrm{d}t}\frac{\partial \mathcal{L}}{\partial \mathbf{q}_i'} - \frac{\partial \mathcal{L}}{\partial \mathbf{q}_i} = \mathbf{0}, \quad \frac{\mathrm{d}}{\mathrm{d}t}\frac{\partial \mathcal{L}}{\partial \mathbf{H}_i'} - \frac{\partial \mathcal{L}}{\partial \mathbf{H}_i} = \mathbf{0} \tag{2.36}$$

are derived from this Lagrange-function. With the normalized forces

$$\mathbf{F}_i = -\frac{1}{m_i}\frac{\partial V}{\partial \mathbf{q}_i}, \quad \mathbf{M}_i = -\frac{1}{m_i}\frac{\partial V}{\partial \mathbf{H}_i} \tag{2.37}$$

explicitly given by

$$\mathbf{F}_i = -\int \Big\{ \frac{\partial \varepsilon}{\partial \rho} + S_i \frac{\partial \varepsilon}{\partial s} \Big\} \frac{\partial \psi_i}{\partial \mathbf{q}_i}\, \mathrm{d}\mathbf{x}, \tag{2.38}$$

$$\mathbf{M}_i = -\int \Big\{ \frac{\partial \varepsilon}{\partial \rho} + S_i \frac{\partial \varepsilon}{\partial s} \Big\} \frac{\partial \psi_i}{\partial \mathbf{H}_i}\, \mathrm{d}\mathbf{x}, \tag{2.39}$$

these equations read

$$\mathbf{q}_i'' = \mathbf{F}_i\,, \quad \mathbf{H}_i'' = \frac{1}{J}\,\mathbf{M}_i. \tag{2.40}$$

Note that the masses m_i of the particles cancel out and appear only implicitly in the mass density ρ and the entropy density s. The derivatives of ψ_i occurring in the expressions above can be written as functions of the internal particle coordinates (2.9) and are given by (2.19). The pressure forces (2.37) acting upon a group of particles can be interpreted as a kind of surface force [11].

As long as the specific entropies S_i of the single particles are assumed to be constant, the time evolution of the system is completely determined by the equations of motion (2.36). This system is time reversible, a fact that contradicts the behavior of actual fluids where heat is generated in shock fronts. Therefore it has been proposed in [13] to add the (normalized) frictional force

$$\mathbf{F}_i^{(r)} = -\frac{1}{2}\int R\,\psi_i\,[\,\mathbf{v}_i - \mathbf{v}\,]\,\mathrm{d}\mathbf{x} \tag{2.41}$$

to the right-hand side of the first equation in (2.40). This force damps local velocity fluctuations and couples the particles softly together. The difference between the velocity of the given particle and the velocity field of the surrounding flow determines the direction of the force and the scalar function $R \geq 0$ its size. The quantity in the equation for the $\mathbf{H}_i$ corresponding to the force (2.41) is

$$\mathbf{M}_i^{(r)} = -\frac{1}{2}\int R\,\psi_i\,[\,\mathbf{v}_i - \mathbf{v}\,][\,\mathbf{H}_i^{-1}(\mathbf{x} - \mathbf{q}_i)\,]^{\mathrm{T}}\,\mathrm{d}\mathbf{x}. \tag{2.42}$$

In smooth flows, the forces (2.41) and (2.42) will be comparatively small and will vanish with the second power of the local particle size, but they can dominate in shocks.

For a better quantitative understanding of the frictional forces (2.41), (2.42), we pause for a moment and consider a little model problem. We neglect the pressure forces, keep R constant, and fix the velocity field $\mathbf{v} = \mathbf{0}$. The equations of motion for a single particle then read

$$\mathbf{q}'' = -\frac{R}{2}\,\mathbf{q}', \quad \mathbf{H}'' = -\frac{R}{2}\,\mathbf{H}';$$

that is, within the time $T = 2/R$, the velocity of the particle is reduced by the factor $1/\mathrm{e}$. This justifies calling $T = 2/R$ the local relaxation time of the system. With $\mathbf{q}'(t_0) = \mathbf{v}_0$, the trajectory of the particle is

$$\mathbf{q}(t) = \mathbf{q}(t_0) + \Big(1 - \exp\Big(\frac{t_0 - t}{T}\Big)\Big) T\mathbf{v}_0.$$

Thus the particle is stopped in distance $T|\mathbf{v}_0|$ from its position at the given time t_0.

The friction among the particles generates heat. Therefore the specific entropies S_i are no longer constant and increase in time. They obey the differential equations

$$\theta_i(t) S_i'(t) = \delta Q_i(t). \tag{2.43}$$

The quantity θ_i defined by

$$\theta_i = \frac{1}{m_i}\frac{\partial V}{\partial S_i} \tag{2.44}$$

is the mean value

$$\theta_i(t) = \int \theta(\rho(\mathbf{x},t), s(\mathbf{x},t))\,\psi_i(\mathbf{x},t)\,\mathrm{d}\mathbf{x} \tag{2.45}$$

of the absolute temperature around the particle and

$$\delta Q_i^{(r)} = \frac{1}{m_i}\int \chi_i R q\,\mathrm{d}\mathbf{x} \tag{2.46}$$

the specific heat supply. The quantity

$$q = \frac{1}{4}\,\rho \sum_{i,j=1}^{N} \chi_i \chi_j\,|\mathbf{v}_i - \mathbf{v}_j|^2 \geq 0 \tag{2.47}$$

is the density of the fluctuation energy. It can be rewritten as

$$q = \frac{1}{2}\sum_{i=1}^{N} m_i \psi_i |\mathbf{v}_i|^2 - \frac{1}{2}\,\rho\,|\mathbf{v}|^2 \tag{2.48}$$

which is more convenient for computational purposes. Equation (2.43) is the second law of thermodynamics. It ensures conservation of energy as will be shown in section 3. Note that the specific entropy of a particle never decreases.

If the $\mathbf{q}_i$ and $\mathbf{H}_i$ and the function R are kept fixed,

$$\mathbf{q}_i',\ \mathbf{H}_i' \longrightarrow \mathbf{F}_i^{(r)},\ \frac{1}{J}\,\mathbf{M}_i^{(r)} \tag{2.49}$$

is a linear mapping. To study this mapping, we utilize the energy norm given by

$$\mathbf{q}_i',\ \mathbf{H}_i' \ \longrightarrow\ \Big[\ \sum_{i=1}^{N}\Big\{\ \frac{1}{2}m_i|\mathbf{q}_i'|^2+\frac{1}{2}Jm_i|\mathbf{H}_i'|^2\Big\}\Big]^{1/2} \tag{2.50}$$

and the corresponding energy inner product, respectively. Note that the square of the energy norm of the vector consisting of the velocity components $\mathbf{q}_i'$ and $\mathbf{H}_i'$ is the total kinetic energy (2.33) of the system. Denoting by $\widehat{\mathbf{v}}_i$ the velocities (2.16) formed with $\widehat{\mathbf{q}}_i'$ and $\widehat{\mathbf{H}}_i'$ instead of $\mathbf{q}_i'$ and $\mathbf{H}_i'$, one has

$$\sum_{i=1}^{N} m_i\left(\widehat{\mathbf{q}}_i'\cdot\mathbf{F}_i^{(r)}+\widehat{\mathbf{H}}_i'\cdot\mathbf{M}_i^{(r)}\right)\ =\ -\int RQ\,\mathrm{d}\mathbf{x} \tag{2.51}$$

with the symmetric bilinear form

$$Q\ =\ \frac{1}{4}\,\rho\sum_{i,j=1}^{N}\chi_i\chi_j\,[\widehat{\mathbf{v}}_i-\widehat{\mathbf{v}}_j]\cdot[\mathbf{v}_i-\mathbf{v}_j] \tag{2.52}$$

in the velocities $\mathbf{v}_i$ and $\widehat{\mathbf{v}}_i$. This shows that the linear mapping (2.49) is negative semidefinite and self-adjoint with respect to the energy inner product. For R constant, its eigenvalues range in the interval $[-1/T, 0]$. The proof of (2.51) is based on the same arguments as the proof of Theorem 1 below.

In viscous fluids, an additional force

$$\int_{\partial W_t}\mathbf{T}\mathbf{n}\,\mathrm{d}A \tag{2.53}$$

acts upon the mass contained in a volume W_t transported with the flow, that is, the mass initially contained in a given volume $W = W_0$ inside the region occupied by mass. The symmetric tensor $\mathbf{T}$ is the viscous part of the stress tensor and is a function of the density, the temperature, and of the symmetric part

$$\mathbf{D}=\frac{1}{2}\,(\nabla\mathbf{v}+\nabla\mathbf{v}^T) \tag{2.54}$$

of the gradient of the velocity field. In Newtonian fluids, it depends linearly on $\mathbf{D}$ and $\mathbf{v}$, respectively, and is given by

$$\mathbf{T}\ =\ 2\eta\left[\mathbf{D}-\frac{1}{d}(\operatorname{tr}\mathbf{D})\mathbf{I}\right]+\zeta(\operatorname{tr}\mathbf{D})\mathbf{I} \tag{2.55}$$

in d space dimensions. The first term on the right-hand side has trace zero and describes the shear forces in the fluid. The second part comes from the bulk viscosity. The viscosity coefficients η and ζ are nonnegative functions of ρ and θ, which guarantees

$$\mathbf{T}\cdot\mathbf{D}\geq 0\,, \tag{2.56}$$

a fundamental property needed to satisfy the second law of thermodynamics. For most gases, $\zeta = 0$ can be assumed.

To model the viscous forces, one starts from the observation that

$$\int_{\partial W_t} \mathbf{T}\mathbf{n}\,\mathrm{d}A \;=\; -\lim_{\delta\to 0}\int \mathbf{T}\nabla\chi_\delta\,\mathrm{d}V, \tag{2.57}$$

where the χ_δ are continuously differentiable functions with values between 0 and 1 vanishing outside W_t and tending pointwise to the characteristic function of W_t for δ tending to 0. If I denotes the set of indices of the particles initially contained in the region W, the mass fraction

$$\chi_W(\mathbf{x},t) = \sum_{i\in I}\chi_i(\mathbf{x},t) \tag{2.58}$$

serves as our discrete counterpart of the functions χ_δ. This leads to the viscous force

$$-\int \mathbf{T}\nabla\chi_W\,\mathrm{d}V \tag{2.59}$$

acting upon this group of particles, or to the normalized force

$$\mathbf{F}_i^{(v)} = -\frac{1}{m_i}\int \mathbf{T}\nabla\chi_i\,\mathrm{d}\mathbf{x} \tag{2.60}$$

acting upon the particle i, where the integrals extend over the region occupied by mass at the given time t. Note that the expression (2.59) correctly takes into account only that part of the boundary of the moving volume that is touched by mass from its exterior. Therefore the construction also covers the case not directly included above when a part of the boundary of the moving volume belongs to the boundary of the region occupied by mass. The quantities $\mathbf{M}_i$ corresponding to the forces (2.60) are

$$\mathbf{M}_i^{(v)} = -\frac{1}{m_i}\int [\,\mathbf{T}\nabla\chi_i\,][\,\mathbf{H}_i^{-1}(\mathbf{x}-\mathbf{q}_i)\,]^{\mathrm{T}}\,\mathrm{d}\mathbf{x} - \frac{1}{m_i}\int \chi_i\,\mathbf{T}\mathbf{H}_i^{-\mathrm{T}}\,\mathrm{d}\mathbf{x}\,, \tag{2.61}$$

and the additional specific heat supply to the particle i is

$$\delta Q_i^{(v)} = \frac{1}{m_i}\int \chi_i\,\mathbf{T}\cdot\mathbf{D}\,\mathrm{d}\mathbf{x}\,. \tag{2.62}$$

Provided the given particle is located in the interior of the region occupied by mass, the forces (2.60) and (2.61) formally vanish for stress tensors $\mathbf{T}$ of divergence zero, as continuum mechanics requires. The proof is by partial integration, where the second integral on the right-hand side of (2.61) cancels.

The problem with this approach is that, in more than one space dimension, the derivatives of the mass fractions χ_i can have singularities and are not always square integrable. Fortunately, this effect is often compensated by the behavior of $\mathbf{T}$ and the properties of the shape function ψ. Assume that $\mathbf{T}$ is of the form (2.55) and that the viscosity coefficients behave like

$$\eta,\zeta = O(\rho^\alpha)\,,\quad \rho\to 0+\,, \tag{2.63}$$

with $\alpha > 0$. Let the gradient of ψ satisfy the pointwise inverse estimate

$$|(\nabla\psi)(\mathbf{y})| \le C\,|\psi(\mathbf{y})|^{(k-1)/k} \tag{2.64}$$

with $k > 1$, as it holds for the cubic splines (2.3), (2.6) with $k = 3$. Then there exist constants C_i depending on the number of the locally interacting particles and their mass, size, and shape with

$$\rho^\alpha |\nabla \chi_i|^2 \le C_i \, \rho^{\alpha - 2/k}. \tag{2.65}$$

Provided that $\alpha - 2/k > 0$, this demonstrates that the integrands above are continuous and tend to zero at the points at which ρ tends to zero. Therefore, under the given circumstances, one can refrain from replacing the χ_i by regularized mass fractions as it has been proposed in [11] and [12]. However, our considerations would immediately transfer to this case.

To incorporate heat conduction, the right-hand side of the entropy equation (2.43) has to be supplemented to

$$\delta Q_i \;=\; \delta Q_i^{(r)} + \delta Q_i^{(v)} + \frac{1}{m_i} \int \mathbf{k} \cdot \nabla \chi_i \, \mathrm{d}\mathbf{x}. \tag{2.66}$$

The heat flux vector $\mathbf{k}$ is mostly given by Fourier's law

$$\mathbf{k} = \, - \kappa \, \nabla \theta, \tag{2.67}$$

where the coefficient function $\kappa \ge 0$ is the heat conductivity. For the heat flux to be well defined, $\mathbf{k}$ has to satisfy an estimate similar to the estimate above for the viscosity coefficients.

For the rest of this section, we restrict ourselves to Newtonian fluids (2.55). For given $\mathbf{q}_i$ and $\mathbf{H}_i$, the mapping

$$\mathbf{q}_i', \; \mathbf{H}_i' \;\longrightarrow\; \mathbf{F}_i^{(v)}, \; \frac{1}{J} \, \mathbf{M}_i^{(v)} \tag{2.68}$$

is then linear. Denoting by $\widehat{\mathbf{D}}$ the tensor (2.54) formed with the velocities $\widehat{\mathbf{q}}_i'$, and $\widehat{\mathbf{H}}_i'$ instead of $\mathbf{q}_i'$ and H_i',

$$\sum_{i=1}^{N} m_i \left(\widehat{\mathbf{q}}_i' \cdot \mathbf{F}_i^{(v)} + \widehat{\mathbf{H}}_i' \cdot \mathbf{M}_i^{(v)} \right) \;=\; - \int \mathbf{T} \cdot \widehat{\mathbf{D}} \, \mathrm{d}\mathbf{x} \tag{2.69}$$

holds, with the integrals discretized as described above. Because

$$\mathbf{T} \cdot \widehat{\mathbf{D}} \;=\; 2\eta \left[\mathbf{D} \cdot \widehat{\mathbf{D}} - \frac{1}{d} \, (\operatorname{tr} \mathbf{D})(\operatorname{tr} \widehat{\mathbf{D}}) \right] + \zeta (\operatorname{tr} \mathbf{D})(\operatorname{tr} \widehat{\mathbf{D}}), \tag{2.70}$$

this proves that also the linear mapping (2.68) is symmetric and negative semidefinite with respect to the energy inner product given by (2.50). For the proof of (2.69), we refer again to the proof of Theorem 1 below.

3. The conservation of energy, momentum, and angular momentum. The conservation of energy, momentum, and angular momentum are basic physical properties of any closed system and must therefore be reproduced by the finite mass method. Moreover, energy estimates are basic for the mathematical examination of the model and, in particular, are needed to transfer the compactness and convergence results from [11] and [13] to the present situation of particles underlying arbitrary linear deformations. The conservation of energy also prevents the determinants of

the $\mathbf{H}_i$ from becoming arbitrarily small since, with equations of state like (2.30), this would require too much energy. Our first result is as follows.

THEOREM 1. *The total energy $\mathcal{E} = E + V$ composed of the kinetic energy* (2.33) *of the particles and the internal energy* (2.34) *is a constant of motion.*

Proof. Utilizing the representation (2.32) of the kinetic energy of a single particle, one first obtains

$$\frac{\mathrm{d}}{\mathrm{d}t}\,(E+V) \;=\; \sum_{i=1}^{N} \big(\, m_i \mathbf{q}_i' \cdot \mathbf{q}_i'' + J m_i \mathbf{H}_i' \cdot \mathbf{H}_i'' \,\big) \\ + \sum_{i=1}^{N} \left(\frac{\partial V}{\partial \mathbf{q}_i} \cdot \mathbf{q}_i' + \frac{\partial V}{\partial \mathbf{H}_i} \cdot \mathbf{H}_i' + \frac{\partial V}{\partial S_i}\, S_i' \right).$$

Therefore, the equations of motion yield

$$\frac{\mathrm{d}}{\mathrm{d}t}\,(E+V) \;=\; E_2' + E_3' + \sum_{i=1}^{N} \frac{\partial V}{\partial S_i}\, S_i',$$

where the terms coming from the pressure forces (2.37) have canceled with the corresponding derivatives of V,

$$E_2' \;=\; \sum_{i=1}^{N} m_i \,\big(\, \mathbf{q}_i' \cdot \mathbf{F}_i^{(r)} + \mathbf{H}_i' \cdot \mathbf{M}_i^{(r)} \big)$$

comes from the frictional forces (2.41), (2.42), and

$$E_3' \;=\; \sum_{i=1}^{N} m_i \,\big(\, \mathbf{q}_i' \cdot \mathbf{F}_i^{(v)} + \mathbf{H}_i' \cdot \mathbf{M}_i^{(v)} \big)$$

from the viscous forces (2.60), (2.61).

Before we start calculating E_2' and E_3', we state two simple algebraic relations that are repeatedly used in this section, namely, that

$$\mathbf{A} \cdot \mathbf{B}\mathbf{a}\mathbf{b}^{\mathrm{T}} = \mathbf{A}\mathbf{b} \cdot \mathbf{B}\mathbf{a} \tag{3.1}$$

for all square matrices $\mathbf{A}$ and $\mathbf{B}$ and all vectors $\mathbf{a}$ and $\mathbf{b}$ and that

$$\mathbf{A} \cdot (\mathbf{B}\mathbf{C}) = (\mathbf{A}\mathbf{C}^{\mathrm{T}}) \cdot \mathbf{B} \tag{3.2}$$

for all square matrices $\mathbf{A}$, $\mathbf{B}$, and $\mathbf{C}$.

For example, with $\mathbf{B} = \mathbf{I}$ the first of these two relations yields

$$\mathbf{q}_i' \cdot \mathbf{f} \;+\; \mathbf{H}_i' \cdot \,[\,\mathbf{f}\,][\,\mathbf{H}_i^{-1}(\mathbf{x}-\mathbf{q}_i)\,]^{\mathrm{T}} \;=\; \mathbf{v}_i \cdot \mathbf{f} \tag{3.3}$$

for arbitrary vectors $\mathbf{f}$. Choosing $\mathbf{f} = \mathbf{v}_i - \mathbf{v}$, with (2.41) and (2.42)

$$E_2' \;=\; -\,\frac{1}{2} \sum_{i=1}^{N} m_i \int R\,\psi_i\, \mathbf{v}_i \cdot [\,\mathbf{v}_i - \mathbf{v}\,]\,\mathrm{d}\mathbf{x}$$

follows. Because, by the definition (2.16) of $\mathbf{v}$,

$$\frac{1}{2} \sum_{i=1}^{N} m_i \psi_i\, \mathbf{v}_i \cdot [\,\mathbf{v}_i - \mathbf{v}\,] \;=\; \frac{1}{2} \sum_{i=1}^{N} m_i \psi_i |\mathbf{v}_i|^2 - \frac{1}{2}\,\rho\,|\mathbf{v}|^2$$

with (2.48) this leads to the representation

$$E_2' \;=\; -\int Rq\,\mathrm{d}\mathbf{x}$$

of the first of the two terms above. Inserting $\mathbf{T}\nabla\chi_i$ for $\mathbf{f}$ in (3.3), one finds

$$E_3' \;=\; -\sum_{i=1}^{N}\left(\int \mathbf{v}_i\cdot\mathbf{T}\nabla\chi_i\,\mathrm{d}\mathbf{x}\;+\int \chi_i\mathbf{H}_i'\cdot\mathbf{T}\mathbf{H}_i^{-\mathrm{T}}\,\mathrm{d}\mathbf{x}\right)$$

for the second part coming from the viscous forces (2.60) and (2.61). As

$$\sum_{i=1}^{N}\mathbf{v}_i\cdot\mathbf{T}\nabla\chi_i \;=\; \mathbf{T}\cdot\mathbf{D}\;-\;\sum_{i=1}^{N}\chi_i\mathbf{T}\cdot\nabla\mathbf{v}_i$$

by the symmetry of $\mathbf{T}$ and

$$\mathbf{T}\cdot\nabla\mathbf{v}_i \;=\; \mathbf{T}\cdot\mathbf{H}_i'\mathbf{H}_i^{-1} \;=\; \mathbf{H}_i'\cdot\mathbf{T}\mathbf{H}_i^{-\mathrm{T}},$$

by the definition of $\mathbf{v}_i$ and (3.2), the second integral in the formula above cancels and the sum attains the value

$$E_3' \;=\; -\int \mathbf{T}\cdot\mathbf{D}\,\mathrm{d}\mathbf{x}.$$

As by (2.43), (2.44), (2.46), (2.62), and (2.66)

$$\sum_{i=1}^{N}\frac{\partial V}{\partial S_i}\,S_i' \;=\; \int Rq\,\mathrm{d}\mathbf{x}\;+\int \mathbf{T}\cdot\mathbf{D}\,\mathrm{d}\mathbf{x},$$

this proves the proposition and demonstrates that exactly the right amount of kinetic energy is converted to heat. □

Surprisingly, for vanishing frictional and viscous forces, one has both conservation of energy and entropy, which contradicts the usual conception of gas flows and would not be possible in continuum mechanics, but which is explained by the fact that the kinetic energy (2.33) considered here is composed of the kinetic energies of the single particles and is not identical with the mean kinetic energy

$$\bar{E}(t) \;=\; \frac{1}{2}\int \rho(\mathbf{x},t)|\mathbf{v}(\mathbf{x},t)|^2\,\mathrm{d}\mathbf{x} \tag{3.4}$$

known from continuum mechanics; it consists additionally of the local fluctuation energy

$$\bar{\bar{E}} \;=\; \frac{1}{4}\int \rho\sum_{i,j=1}^{N}\chi_i\chi_j\,|\mathbf{v}_i-\mathbf{v}_j|^2\,\mathrm{d}\mathbf{x}. \tag{3.5}$$

In smooth flows, this fluctuation energy is a negligibly small part of the total kinetic energy and will vanish with the fourth power of the particle size, but it can dominate where the particles clash. The role of the frictional forces (2.41) and (2.42) is to convert this kind of fluctuation energy into true internal energy.

The total momentum of the system is defined as

$$\mathbf{P}(t) \,=\, \int \rho(\mathbf{x},t)\mathbf{v}(\mathbf{x},t)\,\mathrm{d}\mathbf{x}. \tag{3.6}$$

Because of (2.1), it has the closed representation

$$\mathbf{P}(t) \,=\, \sum_{i=1}^{N} m_i \mathbf{q}_i'(t). \tag{3.7}$$

THEOREM 2. *The total momentum* (3.6) *is a constant of motion.*

Proof. The representation (3.7) and the equations of motion yield

$$\frac{\mathrm{d}}{\mathrm{d}t}\,\mathbf{P} \,=\, \mathbf{P}_1' + \mathbf{P}_2' + \mathbf{P}_3'$$

with the three parts,

$$\mathbf{P}_1' = \sum_{i=1}^{N} m_i \mathbf{F}_i\,,\;\; \mathbf{P}_2' = \sum_{i=1}^{N} m_i \mathbf{F}_i^{(r)},\;\; \mathbf{P}_3' = \sum_{i=1}^{N} m_i \mathbf{F}_i^{(v)},$$

coming from the pressure forces (2.38), the frictional forces (2.41), and the viscous forces (2.60). With (2.19), the first part reads

$$\mathbf{P}_1' \,=\, \sum_{i=1}^{N} m_i \int \Big\{ \frac{\partial \varepsilon}{\partial \rho} + S_i \frac{\partial \varepsilon}{\partial s} \Big\} \nabla \psi_i \,\mathrm{d}\mathbf{x}.$$

By the definitions (2.10) of the mass density and (2.24) of the entropy density, this means

$$\mathbf{P}_1' \,=\, \int \nabla \varepsilon \,\mathrm{d}\mathbf{x}.$$

As ε, under the given assumptions, is a continuously differentiable function with compact support, this yields $\mathbf{P}_1' = \mathbf{0}$. For $\mathbf{P}_2'$, with (2.41) one obtains

$$\mathbf{P}_2' \,=\, -\,\frac{1}{2} \sum_{i=1}^{N} m_i \int R\,\psi_i\,[\,\mathbf{v}_i - \mathbf{v}\,]\,\mathrm{d}\mathbf{x}.$$

As, by the definition (2.16) of the velocity field $\mathbf{v}$,

$$\sum_i m_i \psi_i\,[\,\mathbf{v}_i - \mathbf{v}\,] \,=\, \mathbf{0},$$

$\mathbf{P}_2' = \mathbf{0}$ follows. As the χ_i form a partition of unity, finally also the part

$$\mathbf{P}_3' \,=\, -\sum_{i=1}^{N} \int \mathbf{T} \nabla \chi_i \,\mathrm{d}\mathbf{x}$$

resulting from the viscous forces vanishes. ∎

Last, we consider the scalar quantities

$$L(t) \;=\; \int \rho(\mathbf{x},t)\,\mathbf{x}\cdot\mathbf{W}\mathbf{v}(\mathbf{x},t)\,\mathrm{d}\mathbf{x} \tag{3.8}$$

with fixed skew-symmetric matrices $\mathbf{W}$, which have, by the definition of $\mathbf{v}$ and because of (2.1) and (2.2), the closed representation

$$L \;=\; \sum_{i=1}^{N} \big(\, m_i\mathbf{q}_i\cdot\mathbf{W}\mathbf{q}_i' \;+\; Jm_i\mathbf{H}_i\cdot\mathbf{W}\mathbf{H}_i' \,\big). \tag{3.9}$$

In three space dimensions, the components of the total angular momentum

$$\mathbf{L}(t) \;=\; \int \rho(\mathbf{x},t)\,\mathbf{x}\times\mathbf{v}(\mathbf{x},t)\,\mathrm{d}\mathbf{x} \tag{3.10}$$

are quantities of this form, and vice versa all quantities of the form (3.8) can be composed of the components of the angular momentum (3.10). Therefore, for the three-dimensional case, the following theorem states that the angular momentum of the system is a constant of motion. In other space dimensions, one gets less or more first integrals, corresponding to the dimension of the space of the skew-symmetric matrices.

THEOREM 3. *For arbitrarily given skew-symmetric matrices* $\mathbf{W}$*, the scalar quantity* L *defined by* (3.8) *is a constant of motion.*

Proof. As $\mathbf{a}\cdot\mathbf{W}\mathbf{a}=0$ for all vectors $\mathbf{a}$ and $\mathbf{A}\cdot\mathbf{W}\mathbf{A}=0$ for all square matrices $\mathbf{A}$, one gets

$$\frac{\mathrm{d}L}{\mathrm{d}t} \;=\; \sum_{i=1}^{N} \big(\, m_i\mathbf{q}_i\cdot\mathbf{W}\mathbf{q}_i'' \;+\; Jm_i\mathbf{H}_i\cdot\mathbf{W}\mathbf{H}_i'' \,\big)$$

from the representation (3.9) of L. The equations of motion therefore yield

$$\frac{\mathrm{d}L}{\mathrm{d}t} \;=\; L_1' + L_2' + L_3'$$

where the first part

$$L_1' \;=\; \sum_{i=1}^{N} m_i \big(\, \mathbf{q}_i\cdot\mathbf{W}\mathbf{F}_i \;+\; \mathbf{H}_i\cdot\mathbf{W}\mathbf{M}_i \,\big)$$

comes from the pressure forces (2.38) and (2.39), the second part

$$L_2' \;=\; \sum_{i=1}^{N} m_i \big(\, \mathbf{q}_i\cdot\mathbf{W}\mathbf{F}_i^{(r)} + \mathbf{H}_i\cdot\mathbf{W}\mathbf{M}_i^{(r)} \big)$$

from the frictional forces (2.41) and (2.42), and the third part

$$L_3' \;=\; \sum_{i=1}^{N} m_i \big(\, \mathbf{q}_i\cdot\mathbf{W}\mathbf{F}_i^{(v)} + \mathbf{H}_i\cdot\mathbf{W}\mathbf{M}_i^{(v)} \big)$$

from the viscous forces (2.60) and (2.61).

We show that each of these three parts vanishes separately. From the representation (2.19) of the partial derivatives of ψ_i, (3.1) and (3.2), and the skew-symmetry of $\mathbf{W}$, first

$$\mathbf{q}_i \cdot \mathbf{W} \frac{\partial \psi_i}{\partial \mathbf{q}_i} \,+\, \mathbf{H}_i \cdot \mathbf{W} \frac{\partial \psi_i}{\partial \mathbf{H}_i} \,=\, \mathbf{W}\mathbf{x} \cdot \nabla \psi_i$$

follows. Thus (2.38) and (2.39) yield

$$L_1' \,=\, -\sum_{i=1}^{N} m_i \int \Big\{ \frac{\partial \varepsilon}{\partial \rho} + S_i \frac{\partial \varepsilon}{\partial s} \Big\} \mathbf{W}\mathbf{x} \cdot \nabla \psi_i \, \mathrm{d}\mathbf{x},$$

or, again taking into account the definitions of ρ and s, summed up

$$L_1' \,=\, -\int \mathbf{W}\mathbf{x} \cdot \nabla \varepsilon \, \mathrm{d}\mathbf{x}.$$

As ε is a continuously differentiable function with compact support, partial integration gives

$$L_1' \,=\, \big(\operatorname{tr} \mathbf{W}\big) \int \varepsilon \, \mathrm{d}\mathbf{x}$$

and therefore $L_1' = 0$, because $\mathbf{W}$ is skew-symmetric. In the same way, (3.1) yields

$$\mathbf{q}_i \cdot \mathbf{W}[\mathbf{v}_i - \mathbf{v}] \,+\, \mathbf{H}_i \cdot \mathbf{W}[\mathbf{v}_i - \mathbf{v}][\mathbf{H}_i^{-1}(\mathbf{x} - \mathbf{q}_i)]^{\mathrm{T}} \,=\, \mathbf{x} \cdot \mathbf{W}[\mathbf{v}_i - \mathbf{v}]$$

and therefore, with (2.41) and (2.42),

$$L_2' \,=\, -\frac{1}{2} \sum_{i=1}^{N} m_i \int R \, \psi_i \, \mathbf{x} \cdot \mathbf{W}[\, \mathbf{v}_i - \mathbf{v} \,] \, \mathrm{d}\mathbf{x}.$$

As, by the definition (2.16) of the velocity field $\mathbf{v}$,

$$\sum_i m_i \psi_i \, [\, \mathbf{v}_i - \mathbf{v} \,] \,=\, \mathbf{0},$$

one obtains $L_2' = 0$. With (3.2), the symmetry of the viscous stress tensor $\mathbf{T}$ and the skew-symmetry of $\mathbf{W}$ give

$$\mathbf{H}_i \cdot \mathbf{W}\mathbf{T}\mathbf{H}_i^{-\mathrm{T}} = \mathbf{I} \cdot \mathbf{W}\mathbf{T} \,=\, 0,$$

and therefore, as above,

$$L_3' \,=\, -\sum_{i=1}^{N} \int \mathbf{x} \cdot \mathbf{W}\mathbf{T} \nabla \chi_i \, \mathrm{d}\mathbf{x}.$$

As the χ_i form a partition of unity, finally also $L_3' = 0$. ∎

4. The discretization of the integrals. Our particle model of compressible fluids is purely Lagrangian. It is invariant to arbitrary translations and rotations and, as it concerns the shape the particles can attain, even to every linear transformation of space. These properties must be reflected by the quadrature formula needed to evaluate the integrals that define the forces acting upon the particles.

We start from the observation that the integral of a scalar or vector function f weighted by the mass density (2.10) can be written as a sum

$$\int f\rho \,\mathrm{d}\mathbf{x} \;=\; \sum_{j=1}^{N} m_j \int f(\mathbf{q}_j + \mathbf{H}_j\mathbf{y})\psi(\mathbf{y})\,\mathrm{d}\mathbf{y} \tag{4.1}$$

of contributions from the single mass packets. The integrals on the right-hand side of (4.1) live on the reference domain on which the shape function ψ is strictly positive. They are replaced by a fixed quadrature formula

$$\int g(\mathbf{y})\psi(\mathbf{y})\,\mathrm{d}\mathbf{y} \;\to\; \sum_{\nu=1}^{n} \alpha_\nu g(\mathbf{a}_\nu) \tag{4.2}$$

with weights $\alpha_\nu > 0$ and nodes $\mathbf{a}_\nu$ inside the support of the shape function ψ, which is considered as the weight function here. This results in the composite rule

$$\int f\rho \,\mathrm{d}\mathbf{x} \;\to\; \sum_{j=1}^{N} m_j \left[\sum_{\nu=1}^{n} \alpha_\nu f(\mathbf{q}_j + \mathbf{H}_j\mathbf{a}_\nu)\right] \;=:\; \int f \,\mathrm{d}\mu \tag{4.3}$$

with weights $m_j\alpha_\nu$ and nodes $\mathbf{q}_j + \mathbf{H}_j\mathbf{a}_\nu$, a quadrature rule which is based on the given discretization of mass and not on a subdivision of space into elementary cells. Therefore it has the desired invariance properties.

Utilizing the quadrature rule (4.3), one replaces the potential energy (2.34) by the fully discrete expression

$$V \;=\; \int \tilde{\varepsilon}(\rho, s)\,\mathrm{d}\mu, \tag{4.4}$$

where $\tilde{\varepsilon} = \varepsilon/\rho$ denotes the specific internal energy. With this discrete potential, the normalized forces

$$\mathbf{F}_i = \;-\frac{1}{m_i}\frac{\partial V}{\partial \mathbf{q}_i}, \quad \mathbf{M}_i = \;-\frac{1}{m_i}\frac{\partial V}{\partial \mathbf{H}_i} \tag{4.5}$$

and the temperatures

$$\theta_i = \frac{1}{m_i}\frac{\partial V}{\partial S_i} \tag{4.6}$$

are formed. As both the specific internal energy itself and the quadrature points depend on the $\mathbf{q}_i$ and $\mathbf{H}_i$, the forces $\mathbf{F}_i$ and $\mathbf{M}_i$ correspondingly split into two parts,

$$\mathbf{F}_i = \mathbf{F}_i^{(1)} + \mathbf{F}_i^{(2)}, \quad \mathbf{M}_i = \mathbf{M}_i^{(1)} + \mathbf{M}_i^{(2)}, \tag{4.7}$$

that are of different structure. Into

$$\mathbf{F}_i^{(1)} = \;-\int \Big\{\frac{\partial\tilde{\varepsilon}}{\partial\rho} + S_i\frac{\partial\tilde{\varepsilon}}{\partial s}\Big\}\frac{\partial\psi_i}{\partial\mathbf{q}_i}\,\mathrm{d}\mu, \tag{4.8}$$

$$\mathbf{M}_i^{(1)} = \;-\int \Big\{\frac{\partial\tilde{\varepsilon}}{\partial\rho} + S_i\frac{\partial\tilde{\varepsilon}}{\partial s}\Big\}\frac{\partial\psi_i}{\partial\mathbf{H}_i}\,\mathrm{d}\mu \tag{4.9}$$

TABLE 1
The basic one-dimensional quadrature rule for cubic B-splines.

Nodes	$-\frac{2}{3}$	$-\frac{1}{3}$	0	$\frac{1}{3}$	$\frac{2}{3}$
Weights	$\frac{41}{1280}$	$\frac{316}{1280}$	$\frac{566}{1280}$	$\frac{316}{1280}$	$\frac{41}{1280}$

all quadrature points $\mathbf{q}_j+\mathbf{H}_j\mathbf{a}_\nu$ contained in the support of the given particle i enter, whereas

$$\mathbf{F}_i^{(2)} = -\sum_{\nu=1}^{n} \alpha_\nu \, (\nabla\tilde{\varepsilon})(\mathbf{q}_i+\mathbf{H}_i\mathbf{a}_\nu) \tag{4.10}$$

and the corresponding term

$$\mathbf{M}_i^{(2)} = -\sum_{\nu=1}^{n} \alpha_\nu \, [\,(\nabla\tilde{\varepsilon})(\mathbf{q}_i+\mathbf{H}_i\mathbf{a}_\nu)\,][\,\mathbf{a}_\nu\,]^{\mathrm{T}} \tag{4.11}$$

are completely determined by the function values and the first order derivatives of the mass density and the entropy density at the quadrature points $\mathbf{q}_i+\mathbf{H}_i\mathbf{a}_\nu$ assigned to the particle i itself. The local temperature (4.6) around the particle i transfers to

$$\theta_i = \int \frac{\partial\tilde{\varepsilon}}{\partial s}\,\psi_i \,\mathrm{d}\mu. \tag{4.12}$$

The forces (4.7) replace the forces (2.38) and (2.39) in the Lagrangian equations of motion (2.36) and (2.40), respectively, and the local temperature (4.6) replaces the local temperature (2.44) in the entropy equation (2.43). Note that, through the assumptions we made on $\varepsilon(\rho, s)$ and because

$$0 < \frac{m_j\alpha_\nu}{\rho(\mathbf{q}_j+\mathbf{H}_j\mathbf{a}_\nu)} \le \frac{\alpha_\nu}{\psi(\mathbf{a}_\nu)} \det\mathbf{H}_j, \tag{4.13}$$

the quantities above behave numerically well. The frictional forces (2.41) and (2.42) and the heat supply (2.46) are directly discretized using the quadrature rule (4.3). For the viscous forces (2.60) and (2.61), the heat supply (2.62) and the heat flux in (2.66) one can proceed correspondingly.

The method reacts sensitively on the choice of the weighted quadrature rule (4.2) for the reference domain. Experience has shown that quite a few quadrature points are needed to exploit the full accuracy of the approach. A too small number of quadrature points leads to instabilities, in particular, when the quadrature points are not properly spaced; a high polynomial accuracy alone does not suffice. For the tensor-product third order B-splines described at the beginning of section 2, we had good experience with the tensor-product counterpart of the one-dimensional quadrature rule given by Table 1. This quadrature formula is exact for fifth order polynomials and assigns 5^2 or $n = 25$ quadrature points to each particle in two space dimensions. The total number of quadrature points $\mathbf{q}_j+\mathbf{H}_j\mathbf{a}_\nu$ entering into the computation for a given particle i depends on the overlap of the B-splines and will generally be much higher, not much less than $4^2 \cdot 25 = 400$ in two space dimensions.

The conservation of energy, momentum, and angular momentum transfers to the present case of discretized integrals. The proofs from the last section can be taken

over with minor changes concerning only the pressure terms. For the proof that the total momentum (3.6) remains a constant of motion, one has only to utilize that

$$\sum_{i=1}^{N} m_i \mathbf{F}_i^{(1)} = \int \nabla\tilde{\varepsilon}\,\mathrm{d}\mu\,, \quad \sum_{i=1}^{N} m_i \mathbf{F}_i^{(2)} = -\int \nabla\tilde{\varepsilon}\,\mathrm{d}\mu$$

such that the quantity

$$\mathbf{P}_1' = \sum_{i=1}^{N} m_i \big(\mathbf{F}_i^{(1)} + \mathbf{F}_i^{(2)}\big)$$

vanishes. In the proof that the quantities (3.8) associated with the angular momentum are constants of motion, the relations

$$\sum_{i=1}^{N} m_i \left(\mathbf{q}_i \cdot \mathbf{W}\mathbf{F}_i^{(1)} + \mathbf{H}_i \cdot \mathbf{W}\mathbf{M}_i^{(1)}\right) = -\int \mathbf{W}\mathbf{x} \cdot \nabla\tilde{\varepsilon}\,\mathrm{d}\mu\,,$$
$$\sum_{i=1}^{N} m_i \left(\mathbf{q}_i \cdot \mathbf{W}\mathbf{F}_i^{(2)} + \mathbf{H}_i \cdot \mathbf{W}\mathbf{M}_i^{(2)}\right) = \int \mathbf{W}\mathbf{x} \cdot \nabla\tilde{\varepsilon}\,\mathrm{d}\mu$$

enter, giving $L_1' = 0$.

The essential idea to compute the forces acting upon the particles is to separate the quadrature points from the particles. This reflects the fact that particles do not interact directly with each other but only with global fields like the mass density or the velocity.

Two different data structures are used. The first data structure is associated with the particles themselves. It contains the fixed particles masses m_i, the values $\mathbf{q}_i$, $\mathbf{H}_i$, $\mathbf{q}_i'$, $\mathbf{H}_i'$, and S_i finally to be determined, and storage for both the local temperatures θ_i and for the forces acting upon the particles and the heat supply to the particles, of course. The second data structure is associated with the quadrature points. First, it contains their positions $\mathbf{x}_Z = \mathbf{q}_i + \mathbf{H}_i\mathbf{a}_\nu$ and the weights $\omega_Z = m_i\alpha_\nu$, and then it contains all necessary global information at $\mathbf{x}_Z$ like the values ρ_Z of the mass density, s_Z of the entropy density, $\mathbf{j}_Z$ of the mass flux density, or $\mathbf{v}_Z$ of the velocity, quantities associated with the viscous stress tensor $\mathbf{T}$, should the occasion arise, and the other field information needed in the computation.

The procedure to compute the integrals involved in the differential equations is then quite simple and consists of three phases. We will describe this procedure only for the inviscid case; the case of additional viscous forces is similar.

In the first phase, the quadrature points are generated and the values ρ_Z of the mass density (2.10), s_Z of the entropy density (2.24), $\mathbf{j}_Z$ of the mass flux density (2.13), and $\widehat{q}_Z$ of the intermediate quantity

$$\widehat{q} = \sum_{i=1}^{N} m_i \psi_i |\mathbf{v}_i|^2, \tag{4.14}$$

as well as the gradients of ρ and s at the quadrature points, are assembled. This is a loop on all particles. In this phase, information is transferred from the particles to the quadrature points.

In the second phase, the values of the derivatives

$$\left(\frac{\partial\tilde{\varepsilon}}{\partial\rho}\right)(\rho_Z, s_Z), \quad \left(\frac{\partial\tilde{\varepsilon}}{\partial s}\right)(\rho_Z, s_Z), \tag{4.15}$$

and, to incorporate the frictional forces (2.41) and (2.42), of

$$\mathbf{v}_Z = \frac{\mathbf{j}_Z}{\rho_Z}, \quad q_Z = \frac{1}{2}\,\widehat{q}_Z - \frac{1}{2}\,\rho_Z|\mathbf{v}_Z|^2, \tag{4.16}$$

are computed. These operations work only on the single quadrature points.

In the final third phase, the discrete integrals determining the forces, the heat supplies, and the local temperatures are computed using the results of phase 1 and phase 2. In this phase, information is transferred from the quadrature points back to the particles.

Phase 1 and phase 3 require an efficient access to the quadrature points contained in the support of a given particle. Search trees can be used for this purpose, which have to be set up after the quadrature points have been generated. The information needed to access the quadrature points $\mathbf{q}_i + \mathbf{H}_i\mathbf{a}_\nu$ assigned to a given particle i has to be stored separately.

5. A time-stepping procedure. The remaining big system of differential equations for the particle positions $\mathbf{q}_i$, the deformation matrices $\mathbf{H}_i$, and the entropies S_i has to be solved numerically. In this section, we present a simple, robust second order method for that which is adapted to the structure of this system and the properties of its solutions. The method has been proposed to us by Lubich [7] and is inspired by the recent work of Hochbruck and Lubich [4] on exponential integrators. Its stability range is de facto independent of the strength of the frictional and viscous forces but shrinks, as with all schemes for this type of equation, when approaching incompressibility.

First, we combine the vectors $\mathbf{q}_i$ and the matrices $\mathbf{H}_i$ to a big vector

$$\mathbf{y} \;\sim\; \mathbf{q}_i,\ \mathbf{H}_i \tag{5.1}$$

of dimension $(d + d^2)N$ and the S_i to a vector $\mathbf{z}$ of dimension N. The system of differential equations (2.40), supplemented by the additional frictional forces (2.41) and (2.42) and the viscous forces (2.60) and (2.61), can then be written in the form

$$\mathbf{y}'' = \mathbf{f}(\mathbf{y}, \mathbf{z}) + \mathbf{A}(\mathbf{y}, \mathbf{z})\mathbf{y}', \tag{5.2}$$

and the entropy equation reads

$$\mathbf{z}' = \mathbf{w}(\mathbf{y}, \mathbf{y}', \mathbf{z}). \tag{5.3}$$

The first term on the right-hand side of (5.2) corresponds to

$$\mathbf{f}(\mathbf{y}, \mathbf{z}) \;\sim\; \mathbf{F}_i,\ \frac{1}{J}\,\mathbf{M}_i, \tag{5.4}$$

with the $\mathbf{F}_i$ and $\mathbf{M}_i$ the discrete counterparts (4.7) of the pressure forces (2.38) and (2.39). The second term

$$\mathbf{A}(\mathbf{y}, \mathbf{z})\mathbf{y}' \;\sim\; \mathbf{F}_i^{(r)} + \mathbf{F}_i^{(v)},\ \frac{1}{J}\left(\mathbf{M}_i^{(r)} + \mathbf{M}_i^{(v)}\right) \tag{5.5}$$

corresponds to the discretized versions of the frictional forces (2.41) and (2.42) and of the viscous forces (2.60) and (2.61) in Newtonian fluids (2.55). The notation (5.5) reflects that these forces depend only linearly on $\mathbf{q}_i'$ and $\mathbf{H}_i'$. As the considerations in section 2 have shown, the matrices $\mathbf{A} = \mathbf{A}(\mathbf{y}, \mathbf{z})$ are symmetric negative semidefinite with respect to the energy inner product determined by (2.50). Finally, the right-hand side of (5.3) corresponds to

$$\mathbf{w}(\mathbf{y}, \mathbf{y}', \mathbf{z}) \;\sim\; \frac{1}{\theta_i}\left(\delta Q_i^{(r)} + \delta Q_i^{(v)}\right) \tag{5.6}$$

with the δQ_i the discretized versions of (2.46) and (2.62), respectively, plus eventually a term coming from heat conduction. This function depends nonlinearly on all its arguments.

The proposed method for the numerical solution of the system (5.2), (5.3) is a leap-frog scheme. To come from the approximations for $\mathbf{y}'$ at time $t_k - \tau/2$ and for $\mathbf{y}$ and $\mathbf{z}$ at time t_k to the new approximations at times $t_k + \tau/2$ and $t_k + \tau$, respectively, one first computes

$$\mathbf{b}_k = \mathbf{f}(\mathbf{y}_k, \mathbf{z}_k) + \mathbf{A}(\mathbf{y}_k, \mathbf{z}_k)\mathbf{y}'_{k-1/2} = \mathbf{f}_k + \mathbf{A}_k\mathbf{y}'_{k-1/2}. \tag{5.7}$$

The new value for the derivative of $\mathbf{y}$ is then

$$\mathbf{y}'_{k+1/2} = \mathbf{y}'_{k-1/2} + \tau\phi_1(\tau\mathbf{A}_k)\mathbf{b}_k, \tag{5.8}$$

and the new value for $\mathbf{y}$ itself is

$$\mathbf{y}_{k+1} = \mathbf{y}_k + \tau\mathbf{y}'_{k+1/2} + \frac{1}{2}\tau^2\phi_0(\tau\mathbf{A}_k)\mathbf{b}_k, \tag{5.9}$$

where ϕ_0 is given by

$$\phi_0(\lambda) = \exp\left(\frac{\lambda}{2}\right)\left[\phi_2(\lambda) - \phi_1\left(\frac{\lambda}{2}\right)\right] \tag{5.10}$$

and ϕ_1 and ϕ_2 are the entire functions

$$\phi_1(\lambda) = \frac{\mathrm{e}^\lambda - 1}{\lambda}, \quad \phi_2(\lambda) = \frac{\mathrm{e}^\lambda - 1 - \lambda}{\lambda^2/2}. \tag{5.11}$$

The new value $\mathbf{z}_{k+1}$ finally is implicitly determined by the equation

$$\mathbf{z}_{k+1} = \mathbf{z}_k + \frac{\tau}{2}\,\mathbf{w}(\mathbf{y}_k, \mathbf{y}'_{k+1/2}, \mathbf{z}_k) + \frac{\tau}{2}\,\mathbf{w}(\mathbf{y}_{k+1}, \mathbf{y}'_{k+1/2}, \mathbf{z}_{k+1}). \tag{5.12}$$

Using the new $\mathbf{b}_{k+1}$ from the next time step, the approximation

$$\mathbf{y}'_{k+1} = \mathbf{y}'_{k+1/2} + \frac{\tau}{2}\,\phi_1\left(\frac{\tau}{2}\mathbf{A}_{k+1}\right)\mathbf{b}_{k+1} \tag{5.13}$$

is obtained at little additional cost. This approximation does not enter into the further computations. The computation starts with the approximation

$$\mathbf{y}'_{1/2} = \mathbf{y}'_0 + \frac{\tau}{2}\,\phi_1\left(\frac{\tau}{2}\mathbf{A}_0\right)\mathbf{b}_0, \quad \mathbf{b}_0 = \mathbf{f}_0 + \mathbf{A}_0\mathbf{y}'_0, \tag{5.14}$$

for $\mathbf{y}'$ at $t_0+\tau/2$ and the approximation

$$\mathbf{y}_1 = \mathbf{y}_0 + \tau\mathbf{y}_0' + \frac{1}{2}\,\tau^2\phi_2(\tau\mathbf{A}_0)\mathbf{b}_0 \tag{5.15}$$

for $\mathbf{y}$ itself at $t_0+\tau$; the quantities $\mathbf{z}_1$ and $\mathbf{y}_1'$ are then computed as above.

The method is constructed such that it would yield the exact values of $\mathbf{y}$ and $\mathbf{y}'$ for $\mathbf{f}$ and $\mathbf{A}$ constant. For vanishing frictional and viscous forces, that is, for $\mathbf{A} = \mathbf{0}$, $\mathbf{w} = \mathbf{0}$, and $\mathbf{f}(\mathbf{y},\mathbf{z}) = \mathbf{f}(\mathbf{y})$, the scheme transfers to the time-reversible integrator

$$\mathbf{y}_{k+1/2}' = \mathbf{y}_{k-1/2}' + \tau\,\mathbf{f}(\mathbf{y}_k), \quad \mathbf{y}_{k+1} = \mathbf{y}_k + \tau\,\mathbf{y}_{k+1/2}' \tag{5.16}$$

known as Verlet method in molecular dynamics, where (5.13) reduces to

$$\mathbf{y}_{k+1}' = \mathbf{y}_{k+1/2}' + \frac{\tau}{2}\,\mathbf{f}(\mathbf{y}_{k+1}). \tag{5.17}$$

With the starting step above, the Verlet method is equivalent to the one-step method

$$\mathbf{y}_{k+1} = \mathbf{y}_k + \tau\,\mathbf{y}_{k+1/2}', \quad \mathbf{y}_{k+1}' = \mathbf{y}_{k+1/2}' + \frac{\tau}{2}\,\mathbf{f}(\mathbf{y}_{k+1}) \tag{5.18}$$

where $\mathbf{y}_{k+1/2}'$ is now considered as the intermediate value

$$\mathbf{y}_{k+1/2}' = \mathbf{y}_k' + \frac{\tau}{2}\,\mathbf{f}(\mathbf{y}_k). \tag{5.19}$$

The Verlet method is symplectic and has therefore very favorable properties for Hamiltonian systems as arising in the present case of pure pressure forces [3]. In particular, it preserves momentum and angular momentum: Let

$$\mathbf{P} = \mathbf{\Sigma}\mathbf{y}', \quad L = \mathbf{y}\cdot\mathbf{\Omega}\mathbf{y}' \tag{5.20}$$

denote the total momentum (3.7) and the scalar quantity (3.9). As $\mathbf{\Omega}$ is a skew-symmetric matrix and

$$\mathbf{\Sigma}\mathbf{f}(\mathbf{y}) = \mathbf{0}, \quad \mathbf{y}\cdot\mathbf{\Omega}\mathbf{f}(\mathbf{y}) = 0 \tag{5.21}$$

by Theorems 2 and 3 and the considerations in section 4, respectively, both quantities retain their value in the transition from one time level to the next.

The matrix-vector products $\phi(\tau\mathbf{A})\mathbf{b}$ can be computed by a Krylov-space method based on the symmetric Lanczos process using the energy inner product. Started with the vector $\mathbf{b}$, after m steps the Lanczos algorithm delivers a matrix $\mathbf{V}$ consisting of m columns orthonormal with respect to this inner product, a symmetric tridiagonal matrix $\mathbf{H}$ of dimension $m\times m$, and a rank one matrix $\mathbf{R}$ such that

$$\mathbf{A}\mathbf{V} = \mathbf{V}\mathbf{H} + \mathbf{R}, \quad \mathbf{A}\mathbf{b} = \mathbf{V}\mathbf{H}\mathbf{e}_1. \tag{5.22}$$

The matrix-vector products are then approximated by

$$\phi(\tau\mathbf{A})\mathbf{b} \approx \mathbf{V}\phi(\tau\mathbf{H})\mathbf{e}_1. \tag{5.23}$$

With a spectral decomposition

$$\mathbf{H} = \mathbf{U}\mathbf{D}\mathbf{U}^{\mathrm{T}}, \quad \mathbf{U}\mathbf{U}^{\mathrm{T}} = \mathbf{I}, \quad \mathbf{D} \text{ diagonal}, \tag{5.24}$$

of the small symmetric tridiagonal matrix $\mathbf{H}$, $\phi(\tau\mathbf{H})$ is given by

$$\phi(\tau\mathbf{H}) = \mathbf{U}\phi(\tau\mathbf{D})\mathbf{U}^{\mathrm{T}}. \tag{5.25}$$

Note that the computation of $\mathbf{Ax}$ corresponds to an evaluation of the discretized frictional forces (2.41) and (2.42) and, if necessary, of the discretized viscous forces (2.60) and (2.61) and can be performed without any explicit knowledge of $\mathbf{A}$. The approximation (5.23) converges very fast for entire functions ϕ, much faster than the conjugate gradient method for the solution of a linear system with the coefficient matrix $\mathbf{I} - \tau\mathbf{A}$; see [4]. Usually, very few Krylov steps suffice.

In the examples presented in the next section, we solved (5.12) approximately by two steps of a simple fixed point iteration. More sophisticated methods will be needed when heat conduction is present.

6. Examples. In this section, we have compiled some two-dimensional examples that exhibit a typical behavior and compare the numerical with the known exact solutions. As shape function ψ of the particles, we have used the bicubic B-spline (2.3), (2.6) together with the 25-point quadrature rule described in section 4.

To find a good approximation of the given initial data, we assume that the region occupied by mass at time $t = 0$ is contained inside an axiparallel rectangle and cover this rectangle by a regular grid of gridsize h. The initial matrices are then $\mathbf{H}_i(0) = 2h\mathbf{I}$, and the initial positions are selected from the gridpoints, that we denote by $\mathbf{x}_k$ here. To determine the particle masses, we first compute the coefficients $a_k \geq 0$ minimizing an appropriately chosen distance between the linear combination

$$\sum_k \frac{a_k}{(2h)^2}\,\psi\Big(\frac{\mathbf{x}-\mathbf{x}_k}{2h}\Big) \tag{6.1}$$

and the given initial mass density ρ, for example, by the projected Gauß–Seidel method. At the points $\mathbf{x}_k$ for which $a_k > 0$, particles with $m_i = a_k$ are located. The remaining gridpoints are ignored in what follows.

The initial velocities can be determined by solving the interpolation problem

$$\sum_i \mathbf{c}_i\,\frac{1}{(2h)^2}\,\psi\Big(\frac{\mathbf{q}_j-\mathbf{q}_i}{2h}\Big) = (\rho\mathbf{v})(\mathbf{q}_j) \tag{6.2}$$

at the particle positions $\mathbf{q}_j = \mathbf{q}_j(0)$. Setting

$$\mathbf{q}_i'(0) = \frac{\mathbf{c}_i}{m_i}\,, \quad \mathbf{H}_i'(0) = \mathbf{0}\,, \tag{6.3}$$

the discrete mass flux will virtually be a fourth order approximation to the continuous mass flux $\rho\mathbf{v}$ at time $t = 0$ for $\rho\mathbf{v}$ sufficiently smooth. The specific entropies $S_i(0)$ are computed in the same way interpolating the entropy density s. The alternative is to choose the initial velocities correspondingly to (2.21) as

$$\mathbf{q}_i'(0) = \mathbf{v}(\mathbf{q}_i(0)), \quad \mathbf{H}_i'(0) = (\nabla\mathbf{v})(\mathbf{q}_i(0))\,\mathbf{H}_i(0), \tag{6.4}$$

which works better with dominating external forces and has the advantage that velocity fields linearly depending on $\mathbf{x}$ like rigid body motions are exactly reproduced.

For reference, we recall the Navier–Stokes equations

$$\frac{\partial \rho}{\partial t} + \operatorname{div}(\rho \mathbf{v}) = 0, \tag{6.5}$$

$$\rho \left\{ \frac{\partial \mathbf{v}}{\partial t} + (\nabla \mathbf{v})\mathbf{v} \right\} = -\nabla \pi + \operatorname{div} \mathbf{T}, \tag{6.6}$$

$$\frac{\partial s}{\partial t} + \operatorname{div}(s\mathbf{v}) = \frac{1}{\theta}\, \mathbf{T} \cdot \mathbf{D} \tag{6.7}$$

that govern the time evolution of a smooth compressible flow in the absence of heat conduction and that transfer to the Euler equations for the inviscid case $\mathbf{T} = \mathbf{0}$. These equations have to be completed by material laws like (2.30) and (2.55) and the basic thermodynamic relation (2.28). Often, the equations are stated in a different but mathematically equivalent form, with (6.6) also written as conservation law and (6.7) replaced by the conservation law for the energy. For the special case of inviscid ideal gases (2.30), the entropy equation (6.7) can be replaced by the equation

$$\frac{\partial \pi}{\partial t} + \mathbf{v} \cdot \nabla \pi + \gamma \pi \operatorname{div} \mathbf{v} = 0 \tag{6.8}$$

coupling pressure and velocity.

6.1. Gas clouds. The first example serves, more or less, as consistency check and shows how accurate the method can be. We reproduce the self-similar solutions

$$\rho(\mathbf{x}, t) = \rho_0 \, \frac{1}{\det \mathbf{H}(t)} \, \Psi\big(|\mathbf{H}(t)^{-1}\mathbf{x}|\big), \quad s(\mathbf{x}, t) = 0, \tag{6.9}$$

$$\mathbf{v}(\mathbf{x}, t) = \mathbf{H}'(t)\mathbf{H}(t)^{-1}\mathbf{x} \tag{6.10}$$

of finite mass of the Euler equations. The functions (6.9), (6.10) satisfy the continuity equation (6.5), regardless of the choice of the density profile Ψ, the matrix function $\mathbf{H}(t)$. The entropy equation (6.7) is trivially satisfied. Starting from the internal energy of a barytropic ideal gas (2.30), the momentum equation (6.6) reads

$$\rho_0 \, \frac{\Psi(\xi)}{H} \, \mathbf{H}''\mathbf{H}^{-1}\mathbf{x} = -\pi_0 \, \frac{1}{H^\gamma} \, \frac{\gamma \, \Psi(\xi)^{\gamma-1}\Psi'(\xi)}{\xi} \, \mathbf{H}^{-\mathrm{T}}\mathbf{H}^{-1}\mathbf{x}, \tag{6.11}$$

where $\xi = |\mathbf{H}^{-1}\mathbf{x}|$ has been set and H is an abbreviation for the determinant of $\mathbf{H}$. Up to normalization,

$$\Psi(\xi) = \begin{cases} (1-\xi^2)^{\frac{1}{\gamma-1}}, & 0 \le \xi < 1, \\ 0, & 1 \le \xi \end{cases} \tag{6.12}$$

is the only function with compact support that satisfies the relation (6.11) for an appropriately chosen function $\mathbf{H}(t)$. For $1 < \gamma < 2$, the function (6.12) is continuously differentiable at $\xi = 1$. The corresponding matrix functions $\mathbf{H}(t)$ are the solutions of the differential equation

$$\mathbf{H}''(t) = \frac{2\gamma}{\gamma-1} \frac{\pi_0}{\rho_0} \Big(\frac{1}{\det \mathbf{H}(t)}\Big)^{\gamma-1} \mathbf{H}(t)^{-\mathrm{T}} \tag{6.13}$$

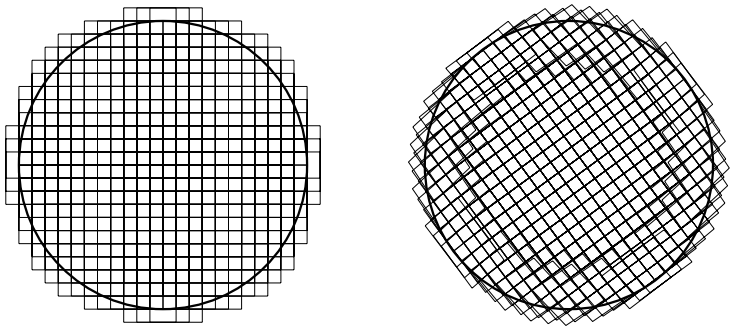

FIG. 1. *The particles in the gas cloud example at times* $t = 0$ *and* $t = 100$.

with initial values $\det \mathbf{H}(0) > 0$. This differential equation coincides with the differential equation from (2.40) that one would obtain for the motion of a single free particle with the shape function (6.12).

If one lets the particles move according to the differential equations (2.21) in the velocity field (6.10), the whole configuration would simply undergo a series of linear transformations. So it is no wonder that a high accuracy can be reached in this example. In the computation presented here, we started from the material constants

$$\gamma = 1.4, \quad \pi_0 = 0.4, \quad \rho_0 = 1, \quad c_v = 10 \tag{6.14}$$

and the initial values

$$\mathbf{H}(0) = \begin{pmatrix} 1 & 0 \\ 0 & 1 \end{pmatrix}, \quad \mathbf{H}'(0) = \begin{pmatrix} -4 & -2 \\ 2 & -4 \end{pmatrix} \tag{6.15}$$

yielding a rotating, first contracting and then again expanding gas ball. The initial positions $\mathbf{q}_i(0)$, the masses m_i, and the matrices $\mathbf{H}_i(0)$ have been determined as described in the introduction to this section. To reproduce the initial velocity field (6.10) exactly, the initial velocities $\mathbf{q}_i'(0)$ and $\mathbf{H}_i'(0)$ have been fixed by (6.4) and not via the linear system (6.2) as in the other examples. The initial entropies are $S_i(0) = 0$. We set $R = 250$ in this example.

We solved the problem over the period $0 \le t \le 100$ with the stepsize $\tau = 1/100$ in the time-stepping procedure from section 4, starting from a grid of gridsize $h = 1/11$ and 21×21 B-splines finally yielding 325 particles. Figure 1 shows the initial configuration of the particles at time $t = 0$ and the final configuration at time $t = 100$, the latter rescaled from the radius determined by (6.13) and (6.15) to the initial radius. The initial configuration of the particles is almost retained over this long period, although the gas ball first shrinks to the radius 0.515 and then again expands to the final radius 516.9, that is, by more than the factor thousand. The exact and the approximate solution cannot be distinguished with the naked eye; the maximum norm of the error is about one per thousand of the maximum norm of the solution. Figure 2 shows a cross section of the mass density together with the differences to the approximate mass densities along the line $x_2 = 2x_1$ at times $t = 0$ and $t = 100$, where all functions are again rescaled to the same radius and the errors have been multiplied by the factor thousand in order to compare them with the exact solution. Astonishingly, the relative size of the error does not increase. One could probably run this example to infinity.

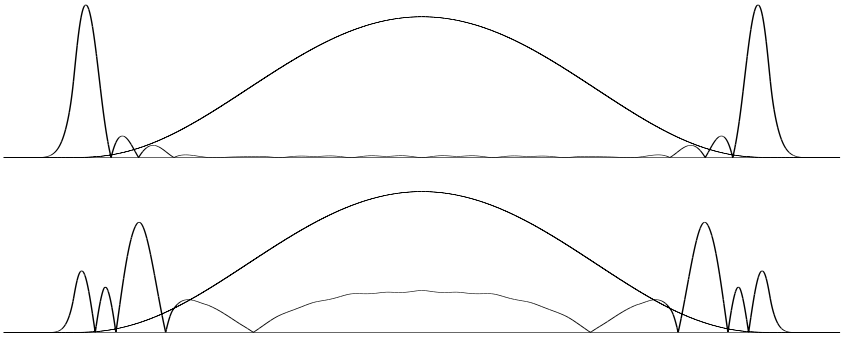

FIG. 2. *Mass density and absolute error in the gas cloud example at times* $t = 0$ *and* $t = 100$.

There is a viscous counterpart of the solutions above, with the same density profile and the viscosity coefficients η and ζ constant multiples of $\theta\rho$. Also these solutions are well reproduced, even if with a slightly reduced accuracy. In examples like these, the shear viscosity must counterbalance the bulk viscosity; otherwise physical instabilities occur.

6.2. Shock fronts. The second example shows how the particle method behaves when shocks develop in an inviscid fluid and demonstrates how the frictional forces (2.41), (2.42) work. In this example, the transformation of kinetic energy into internal energy plays a dominant role.

We consider a spherically symmetric shock front $|\mathbf{x}| = ct$ in an ideal gas (2.30) and make for the velocity, the density, and the pressure the ansatz

$$\mathbf{v}(\mathbf{x},t) = V\Big(\frac{t}{r}\Big)\frac{\mathbf{x}}{r}, \quad \rho(\mathbf{x},t) = M\Big(\frac{t}{r}\Big), \quad \pi(\mathbf{x},t) = P\Big(\frac{t}{r}\Big) \tag{6.16}$$

for $|\mathbf{x}| = r > ct$ and

$$\mathbf{v}(\mathbf{x},t) = \mathbf{0}\,, \quad \rho(\mathbf{x},t) = \rho_1\,, \quad \pi(\mathbf{x},t) = \pi_1 \tag{6.17}$$

with constant values ρ_1 and π_1 for $|\mathbf{x}| < ct$.

To determine the values c, ρ_1, and π_1 and the functions $V(\xi)$, $M(\xi)$, and $P(\xi)$ for $0 \le \xi \le 1/c$ from the initial state

$$\rho_0 = \lim_{t\to 0+} \rho(\mathbf{x},t) = M(0)\,, \quad \pi_0 = \lim_{t\to 0+} \pi(\mathbf{x},t) = P(0)\,, \tag{6.18}$$

and

$$v_0 = -\lim_{t\to 0+} |\mathbf{v}(\mathbf{x},t)| = V(0) < 0\,, \tag{6.19}$$

we first observe that the differential equations (6.5), (6.6), and (6.8) transfer to

$$M\xi V' + (V\xi - 1)M' = (d-1)MV, \tag{6.20}$$

$$(V\xi - 1)MV' + \xi P' = 0, \tag{6.21}$$

$$\gamma P\xi V' + (V\xi - 1)\,P' = (d-1)\gamma PV, \tag{6.22}$$

where d is again the space dimension. For $d > 1$, these differential equations can be used to compute V, M, and P numerically. For $d = 1$, V, M, and P remain constant.

The next step is to express c, ρ_1, and π_1 as functions of the values

$$v_2 = V(1/c)\,, \quad \rho_2 = M(1/c)\,, \quad \pi_2 = P(1/c) \tag{6.23}$$

kept fixed for the time being. Let $u_1 = -c$ and $u_2 = v_2 - c$ be the radial components of the velocity on both sides of the shock front relative to the velocity of the front itself. As continuum mechanics teaches (see [1], for example), the mass flux, the momentum flux, and the energy flux across the shock front are continuous. This is equivalent to the relations

$$\rho_1 u_1 \;=\; \rho_2 u_2\,, \tag{6.24}$$

$$\pi_1 + \rho_1 u_1^2 \;=\; \pi_2 + \rho_2 u_2^2\,, \tag{6.25}$$

$$\left(\frac{1}{2}\rho_1 u_1^2 + \varepsilon_1 + \pi_1\right) u_1 \;=\; \left(\frac{1}{2}\rho_2 u_2^2 + \varepsilon_2 + \pi_2\right) u_2\ . \tag{6.26}$$

With help of (6.24) and (6.25), (6.26) can be replaced by the Hugoniot equation

$$\left(\frac{\varepsilon_2}{\rho_2} - \frac{\varepsilon_1}{\rho_1}\right) + \frac{\pi_1 + \pi_2}{2}\left(\frac{1}{\rho_2} - \frac{1}{\rho_1}\right) \;=\; 0 \tag{6.27}$$

that equivalently expresses the conservation of energy.

For an ideal gas (2.30), the pressure and the internal energy are coupled by the equation of state

$$\pi(\rho, s) = (\gamma - 1)\,\varepsilon(\rho, s). \tag{6.28}$$

The conservation of mass (6.24) leads to

$$\rho_1 \;=\; \left(1 - \frac{v_2}{c}\right)\,\rho_2, \tag{6.29}$$

and with (6.28), the Hugoniot equation (6.27) takes the form

$$\pi_1 \;=\; \frac{(\gamma+1)\,\rho_1 - (\gamma-1)\,\rho_2}{(\gamma+1)\,\rho_2 - (\gamma-1)\,\rho_1}\,\pi_2. \tag{6.30}$$

Inserting (6.29) and (6.30) into (6.25), one finally obtains a quadratic equation for the velocity of the shock front. Only the positive solution

$$c \;=\; -\,\frac{\gamma-3}{4}\,v_2 \;+\; \left[\gamma\,\frac{\pi_2}{\rho_2} \;+\; \left(\frac{\gamma+1}{4}\right)^2 v_2^2\right]^{1/2} \tag{6.31}$$

of this equation is of interest; the negative solution leads to a rarefraction shock that is not compatible with the second law of thermodynamics.

Taking into account the functional dependence (6.23), (6.31) represents an equation for the unknown velocity c and the corresponding value $\xi = 1/c$, respectively. This equation can be solved numerically. With (6.29) and (6.30), one then yields also the values ρ_1 and π_1 for the density and the pressure inside the shock. As an example, with $\gamma = 1.4$ for

$$\rho_0 = 1\,, \quad \pi_0 = 1\,, \quad v_0 = -1 \tag{6.32}$$

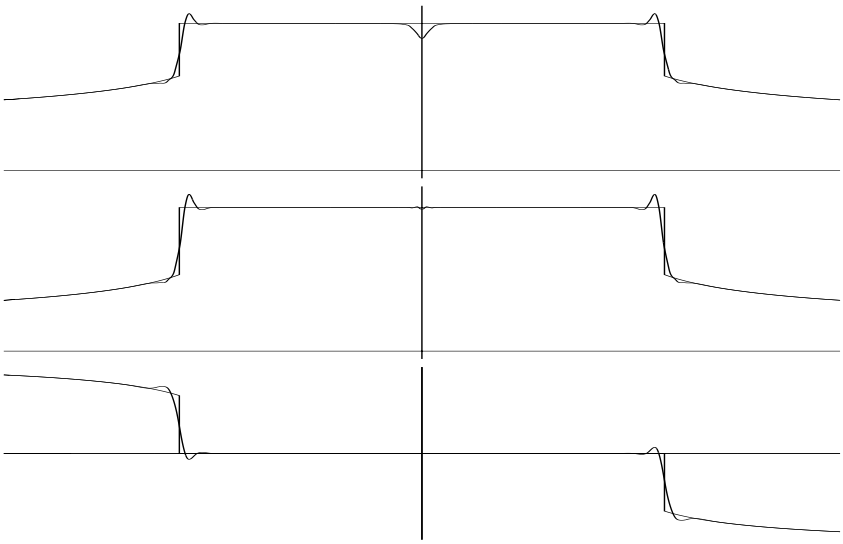

FIG. 3. *Density, pressure, and the velocity in the shock front example at time* $t = 1$.

one obtains

$$c = 1.160\,, \quad \rho_1 = 3.181\,, \quad \pi_1 = 5.105 \tag{6.33}$$

in two space dimensions. The values (6.32) mean that, at time $t = 0$, the fluid collides in the origin with nearly the double speed of sound, which takes the value $\sqrt{\gamma} = 1.183$ here.

We set $R = 250\rho$ in this example. The idea behind this form of R is that friction should grow when the density of matter increases, as physical intuition suggests. In our actual computation we placed 251×251 particles on a regular grid covering the square $[-5, 5]^2$ and followed their motion in the time interval $0 \le t \le 1$. Approximately 10000 of these particles are contained in the region $[-2, 2]^2$ of interest here at time $t = 0$, and slightly more than 20000 at time $t = 1$. With the time stepsize $\tau = 1/200$, the exponential integrator needed 955 Krylov steps, at most 5 for each of the 200 time steps, a typical behavior also observed in other examples.

Figure 3 shows a cross section of the exact and the approximate solution along the x_1-axis on the interval $-2 \le x_1 \le 2$ and Figure 6.2 the corresponding contour lines of the approximate density at time $t = 1$. Both the position and the height of the shock and the solution profile outside the shock are very well reproduced, and the approximate solution retains its spherical symmetry. The shock is practically as well resolved as possible with particles of the given size, and as a closer look at the results of the single time steps shows, the shock does not smear during the computation. Except for the shock region itself and a small neighborhood of the origin, the error of density and pressure is less than one per thousand. The same holds for the velocity field outside the shock. When passing the shock, the particles almost lose all their kinetic energy such that the velocity is practically zero inside the shock. The error in the mass density around the origin is probably due to the discontinuous initial data; the region over which this error extends seems to shrink proportionally to the particle size. An interesting observation is that behind the shock the particles again rearrange to a rectangular grid, as can be seen in Figure 6.2.

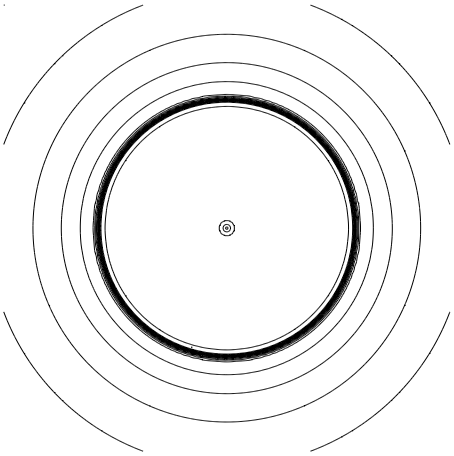

FIG. 4. *Contour lines of the density in the shock front example at time* $t = 1$.

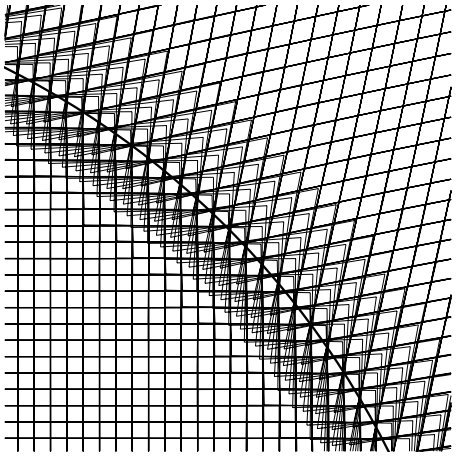

FIG. 5. *Particle contours in a neighborhood of the shock.*

6.3. Shear flows. Our last example serves as a test for the modeling of the shear viscosity. We keep the mass density and the pressure

$$\rho(\mathbf{x}, t) = \rho_0\,, \quad \pi(\mathbf{x}, t) = \pi_0 \tag{6.34}$$

constant, neglect the heat production, that is, set the right-hand side of (6.7) to zero, and consider velocity fields of the form

$$\mathbf{v}(\mathbf{x}, t) = \phi(\xi)c(t)\,\mathbf{n}, \tag{6.35}$$

where $\mathbf{n}$ is a given unit vector fixing the direction of the flow and $\xi = \mathbf{e} \cdot \mathbf{x}$ the component of $\mathbf{x}$ in direction of a unit vector $\mathbf{e}$ orthogonal to $\mathbf{n}$. Again, the continuity equation is fulfilled independent of the choice of the functions ϕ and c. For a Newtonian fluid (2.55) with constant shear viscosity η, the momentum equation (6.6) reads

$$\rho_0\phi(\xi)c'(t)\,\mathbf{n} = \eta\,\phi''(\xi)c(t)\,\mathbf{n}. \tag{6.36}$$

This means that either $\phi(\xi)$ is linear and $c(t)$ constant, that is,

$$\mathbf{v}(\mathbf{x}, t) = \xi\, v_0\mathbf{n} \tag{6.37}$$

up to a translation in direction of $\mathbf{e}$, or correspondingly

$$\mathbf{v}(\mathbf{x}, t) = \sin\Big(\frac{\xi}{L}\Big)\exp\Big(-\frac{t}{T}\Big)\,v_0\mathbf{n} \tag{6.38}$$

with $L > 0$ and v_0 given and $T = L^2\rho_0/\eta$.

The solution corresponding to the velocity field (6.37) is remarkable in so far as it is reproduced exactly provided that the initial data are exact and the integrals defining the forces are evaluated exactly. The reason is that all forces acting upon the particles then vanish such that all particles are distorted in the same way and mass density and pressure remain constant.

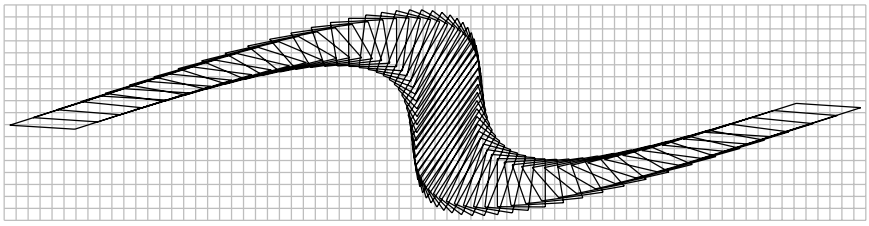

FIG. 6. *The deformation of particles in the shear flow example.*

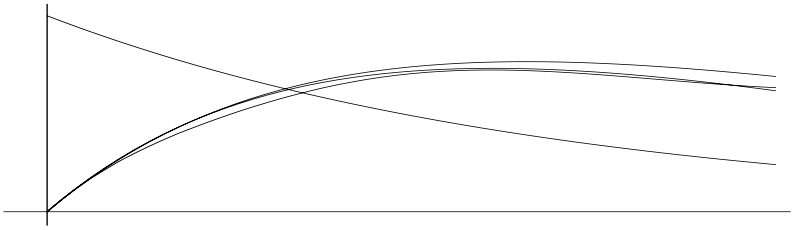

FIG. 7. *The time evolution of the velocity and the rescaled errors in the shear flow example.*

The solution with the velocity field (6.38) represents a more severe test. If one lets the particles move according to the differential equations (2.21) in the velocity field (6.38), the particle positions $\mathbf{q}_i$ and the matrices $\mathbf{H}_i$ at time t would be

$$\mathbf{q}_i(t) = \mathbf{q}_i(0) + \alpha(t)\mathbf{q}_i'(0), \quad \mathbf{H}_i(t) = \mathbf{H}_i(0) + \alpha(t)\mathbf{H}_i'(0) \tag{6.39}$$

with the function $\alpha(t)$ given by

$$\alpha(t) = \Big(1 - \exp\Big(-\frac{t}{T}\Big)\Big)\, T. \tag{6.40}$$

Thus, in a little while, the particles have practically lost all their kinetic energy and get stuck.

In our experiments, we used the data

$$\gamma = 1.4, \quad \pi_0 = 0.4, \quad \rho_0 = 1, \quad c_v = 10, \quad \eta = 0.1 \tag{6.41}$$

fixing the physical properties of the fluid, set $v_0 = 1$, and choose $R = 250$ as in the first example. To exclude influences coming from an alignment of the particles with the flow and to avoid problems with the infinite extension of the flow region, we set

$$\mathbf{n} = \frac{1}{\sqrt{13}}\begin{pmatrix}3\\2\end{pmatrix}, \quad L = \frac{6}{2\pi\sqrt{13}}\,. \tag{6.42}$$

The problem then becomes periodic with period interval $[0,3] \times [0,2]$. All computations were for the time interval $0 \le t \le 1$ with time stepsize $\tau = 1/100$.

The particles in Figure 6 stem from such a computation. They have initially been located on an axiparallel grid of sidelength $h = 1/20$. Figure 7 shows how the velocity field and the errors corresponding to the initial gridsizes $h = 1/10$, $h = 1/20$, and $h = 1/40$ evolve in time, where the function values have been sampled on a 500×500 grid and the associated l_2-norm has been taken as distance measure. For

better comparison, the errors have been multiplied by the factors 25, $16 \cdot 25 = 400$, and $16^2 \cdot 25 = 6400$, respectively. The picture demonstrates that the viscous time scale is perfectly reproduced. In the transition from 30×20 to 60×40 and from 60×40 to 120×80 particles, the error decreases approximately by the factor 16, a clear fourth order convergence, and a fine confirmation of the finite mass method.

REFERENCES

[1] A.J. Chorin and J.E. Marsden, *A Mathematical Introduction to Fluid Mechanics*, Springer-Verlag, New York, 1993.

[2] R. Courant and K.O. Friedrichs, *Supersonic Flow and Shock Waves*, Interscience Publishers, New York, 1948.

[3] E. Hairer, S.P. Nørsett, and G. Wanner, *Solving Ordinary Differential Equations*, 1. *Nonstiff Problems*, 2nd ed., Springer-Verlag, Berlin, 1993.

[4] M. Hochbruck and C. Lubich, *On Krylov subspace approximations to the matrix exponential operator*, SIAM J. Numer. Anal., 34 (1997), pp. 1911–1925.

[5] L.D. Landau and E.M. Lifschitz, *Lehrbuch der Theoretischen Physik. Band* I, *Mechanik*, Akademie-Verlag, Berlin, 1990.

[6] L.D. Landau and E.M. Lifschitz, *Lehrbuch der Theoretischen Physik. Band* VI, *Hydrodynamik*, Akademie-Verlag, Berlin, 1991.

[7] C. Lubich, private communication, 1999.

[8] J.J. Monaghan, *Smoothed particle hydrodynamics*, Ann. Rev. Astron. Astrophys., 30 (1992), pp. 543–574.

[9] J.R. Pasta and S. Ulam, *Heuristic numerical work in some problems of hydrodynamics*, Math. Tables Aids Comput., 13 (1959), pp. 1–12.

[10] J. von Neumann, *Proposal and analysis of a new numerical method in the treatment of hydrodynamical shock problems*, in Collected Works, Vol. 6, Pergamon Press, Oxford, 1963, pp. 351–379.

[11] H. Yserentant, *A particle model of compressible fluids*, Numer. Math., 76 (1997), pp. 111–142.

[12] H. Yserentant, *Particles of variable size*, Numer. Math., 82 (1999), pp. 143–159.

[13] H. Yserentant, *Entropy generation and shock resolution in the particle model of compressible fluids*, Numer. Math., 82 (1999), pp. 161–177.

[14] H. Yserentant, *A convergence analysis for the finite mass method for flows in external force and velocity fields*, SIAM J. Numer. Anal., submitted.